Solar Flares and Magnetospheric Particles: Investigations Based Upon the ONR-602 and ONR-604 Experiments

Performance Report

ONR Grant

N00014-90-J-1466

Second Quarter FY94

John P. Wefel and T. Gregory Guzik

Department of Physics and Astronomy
Louisiana State University
Baton Rouge, LA 70803-4001

Phone: 504-388-8696
FAX: 504-388-1222

19 May 1994

"Solar Flares and Magnetospheric Particles: Investigations Based Upon the ONR-602 and ONR-604 Experiments"

I. Introduction:

This performance report covers work accomplished under ONR Grant N00014-90-J-1466 related to the radiation environment in near-Earth space. The goal of the research is to measure and describe, quantitatively, the Geospace radiation environment in which men and spacecraft must survive and function. The tools for this investigation are the data returned by the ONR-602 and ONR-604 experiments, both flown under the auspices of ONR and the Air Force Space Test Program, augmented by correlative databases of both space-based and ground-based data. The investigation involves data analysis, modeling and applications to a variety of space equipment and environments.

This report builds upon the detailed Technical Report (Fall, 1992) and the previous performance reports. For the current period, the principal effort was in analysis of the full set of solar energetic particle (SEP) events, comparing CRRES measured spectra to model calculations and finalizing a manuscript on the "trapped helium" for submission.

II. Solar Energetic Particle Events

In the previous report, we described the full set of SEP events from the CRRES mission. These are derived from Figure 1 which shows the helium counting rate as a function of orbit during the CRRES mission (c.f. Performance report from second quarter FY93). The major SEP events, e.g. March and June 1991 are readily discernible in Figure 1. Note that there are also smaller events for which the increase is a factor of 2-4 above the baseline. It is these smaller flares that have now been isolated and studied in some detail.

Previously we looked at the big flares for both modeling and for information on the $^3He/^4He$ ratios. For the smaller flares, the statistics are too meager for an isotopic analysis, but one can still look at them from the modeling viewpoint. Here the important parameters are the proton and helium energy spectra, the heavy ion enrichment, if any, and the total duration of the event. Average properties are determined by using all of the events that are SEP related. Afterwards, corrections are made for the Galactic Cosmic Ray (GCR) background within the flare period.

For some of the flares early in the mission, there were data coverage gaps that prevented determination of some of the identifying parameters. In particular, not all of these smaller SEP's can be correlated with known flares and may be due to non-flare Coronal Mass Ejections. This accounts for the identification gaps in Table 1 which summarizes the twenty-six events that have been isolated. Even if there is some coverage outage, the existing data can still be studied to give, at least, limits on the parameters. In some cases, it is necessary to sum several small events to fit an energy spectrum. In these cases it is assumed that the resulting spectrum applies to each of the events within the sum.

The helium energy spectrum is fit to a power law:

$$\frac{dJ}{dE} = A\,(E/E_0)^{-\gamma} \qquad (1)$$

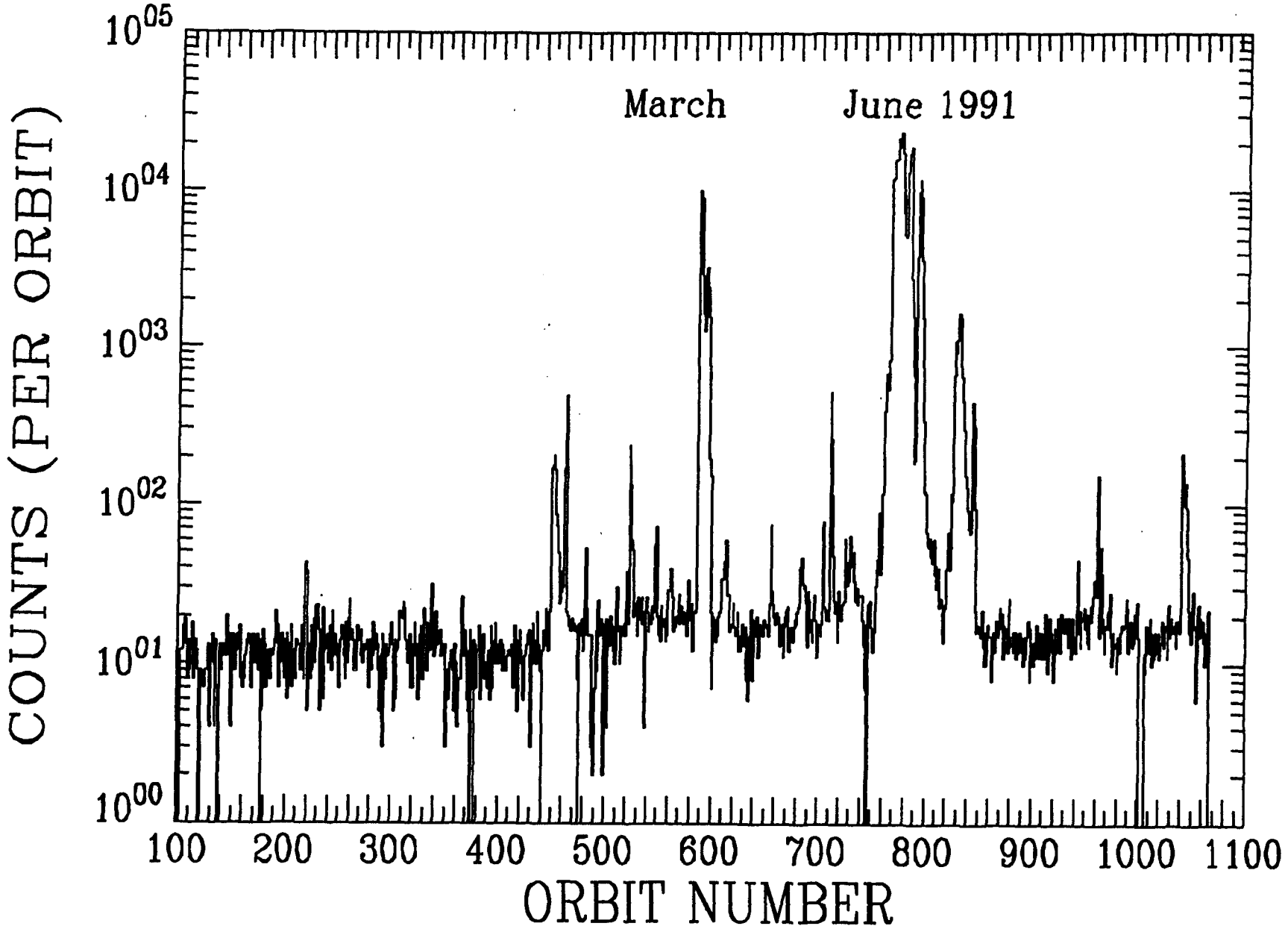

Figure 1. Helium intensity (counts per orbit) observed during the CRRES mission.

Table 1: SEP Events During the CRRES Mission

Event Number	Peak Orbit	Start (Day)	Peak (Day)	End (Day)	Peak He (cnt/orb)	Assoc. Flare (Day/UT)	Imp. X-ray/H_α	Location	Region Number
1	–	207.7/90	208.0	209.5/90	–	–	–	–	–
2	–	213.0/90	213.8	214.9/90	–	Jul30/0736	M4/2B	N20E45	6180
3	218	296.5/90	296.7	297.6/90	43	–	–	–	–
4	451	26.0/91	27.2	29.3/91	201	Jan25/0630	X10/SF	S16E78	6471
5	462	31.3	31.7	32.4	481	Jan31/0230	X1/2B	S17W35	6469
6	481	39.3	39.6	39.9	53	Feb07/1502	M8/1F	S10W86	6471
7	522	56.4	56.5	57.6	235	Feb25/0819	X1/2N	S16W80	6497
8	548	66.4	66.9	67.2	72	Mar07/0748	X5/3B	S20E66	6538
9	562	72.0	72.7	73.0	39	Mar12/1250	X1/2B	S07E59	6545
10	587	82.1	83.1	84.6	9026	Mar22/2247	X9/3B	S26E28	6555
11	593	84.6	85.4	87.6	3234	Mar25/0818	X5/3B	S24W13	6555
12	613	93.0	93.6	94.5	60	Apr02/2327	M6/3B	N14W00	6562
13	655	110.5	110.8	111.2	75	Apr20/0852	X1/3N	N08W50	6583
14	684	122.1	122.6	123.1	46	–	–	–	–
15	704	130.7	130.9	131.7	78	–	–	–	–
16	710	133.1	133.4	135.0	517	May13/0144	M8/–	S09W90	6615
17	730	139.0	141.5	142.9	63	May18/0546	X2/2B	N32W85	6619
18	756	151.2	152.2	153.0	91	May30/0938	M8/1B	N07E30	6654
19	774	153.0	159.6	162.1	23404	Jun04/0352*	X12/3B	N30E70	6659
20	781	162.1	162.6	165.5	13236	Jun11/0209	X12/3B	N31W17	6659
21	791	166.3	166.7	173.6	10101	Jun15/0821	X12/3B	N33W69	6659
22	829	179.5	183.0	188.3	1648	Jun28/0626	M6/–	N30E85	6703
23	843	188.4	189.1	190.3	370	Jul07/0223	X1/2B	N26E03	6703
24	942	231.1	231.5	231.9	45	–	–	–	–
25	961	238.7	239.7	241.4	156	Aug25/0115	X2/2B	N25E64	6810
26	1040	273.0	273.7	276.3	212	Sep29/1533	M7/4B	S21E32	6853

* Event 19 may associate three solar flares peaked at Jun1/1529 (X12/1F, N25E90), Jun4/0352 (X12/3B, N30E70), and Jun6/0112 (X12/4B, N33E44) in the same NOAA region 6659. The source for the flare identification (columns 7, 8, 9, and 10) is from Solar-Geophysical Data books (1991).

with $E_0 = 66$ MeV/nucleon and A the amplitude and γ the spectral index. The best estimates of A and γ are given in columns 2 and 3 of Table 2. The total particle fluence is obtained by integrating over the duration of the event, and this is given, also, along with the event duration, in Table 2.

As we have shown previously, the hydrogen spectra are different from the helium spectra and the time profile of an SEP event may be different for hydrogen and helium. We have utilized GOES and IMP-8 data to determine the proton spectrum, fitting again to a power law such as equation (1). The proton amplitude, spectral index, total fluence and event duration are given in columns 2-5 of Table 3. Comparison of Tables 2 and 3 show that the proton spectra are generally much harder than the helium spectra and, as expected, the total proton fluence is several orders of magnitude larger than the helium results.

We have developed a modeling technique for SEP events which assumes that the heavy ion spectra follow the helium spectrum (not the proton spectrum) with a spectral amplitude determined by the relative coronal abundances of the different species, corrected for any heavy ion enhancement (or deficiency) in the event. To determine such an enrichment parameter, we look at the total heavy ions observed during the flare period by ONR-604. If an enhanced abundance is observed, this is used to define a pseudo-Fe/O ratio which then gives the model parameter δ. Both the Fe/O and δ results are given in Table 3. If no heavy ions are observed, then the Fe/O ratio is set at its nominal value (0.155) and the δ parameter is 0. For these events we assume normal abundances.

It should be remarked that this analysis is at relatively high energy, i.e. 50-100's of MeV/nucleon, where statistics for power-law spectra are poor. Good measurements are obtained for only the largest flares with the smaller flares giving only limits. The range over which the model holds some validity is $E > 10$ MeV/nucleon, the interval that is most important for the Single Event Upset problem in microelectronic circuitry. The present results are not meant to compare to the copious low energy (few MeV/nucleon) results which show a wider range of variation in enrichment parameters. Most of the very small flare events studied at low energies do not give detectable signals at the higher energies investigated by ONR-604.

We can utilize the results of Tables 1-3, within the uncertainties, to look at the probable behavior of the 26 flares that have been studied. Utilizing the model, we can predict the heavy ion spectrum that would be observed with a larger instrument at the energies under consideration here. These results are shown in Figure 2a-m. The left-hand plots show the measured H (solid) and He (dashed) energy spectra while the right-hand graphs show the inferred heavy ion abundance at ~100 MeV/nucleon. The relative importance of the heavy ions can be determined by looking at the ratio between helium and, for example, the CNO peak, considering also the steepness of the helium energy spectrum. A glance through Figure 2a-m shows the variability in the set of SEP events that were encountered, and measured by ONR-604, during the CRRES mission.

The importance of this modeling effort lies in the fact that it is now possible to obtain a representation of the total environment during any sub-interval of the CRRES mission. For a given time period the total SEP fluence of all species can be calculated, and added to the GCR fluence, to look at effects that might be produced in a specific instrument or micro-electronic device. From the point-of-view of SEP physics, the ONR-604 data represents the first study at relatively high energy and, even though it is statistics limited, the ONR-604 provides valuable new data.

Table 2: ^{4}He Spectra and Fluences

Event Number	Amplitude A^*	Index γ	Fluence** (at E_0)	Duration (Days)
1	0.071±0.008	3.27±0.47	1.1×10^4	1.8
2	0.071±0.008	3.27±0.47	1.2×10^4	1.9
3	0.071±0.008	3.27±0.47	6.7×10^3	1.1
4	0.166±0.014	2.22±0.39	4.7×10^4	3.3
5	0.139±0.010	5.43±0.33	1.3×10^4	1.1
6	0.081±0.007	3.21±0.39	4.2×10^3	0.6
7	0.108±0.006	1.54±0.30	1.1×10^4	1.2
8	0.081±0.007	3.21±0.39	5.6×10^3	0.8
9	0.081±0.007	3.21±0.39	7.0×10^3	1.0
10	15.82±0.44	6.33±0.12	3.4×10^6	2.5
11	1.226±0.026	5.07±0.10	3.2×10^5	3.0
12	0.071±0.008	3.27±0.47	9.2×10^3	1.5
13	0.081±0.007	3.21±0.39	4.9×10^3	0.7
14	0.081±0.007	3.21±0.39	7.0×10^3	1.0
15	0.081±0.007	3.21±0.39	7.0×10^3	1.0
16	0.236±0.012	3.31±0.24	3.9×10^4	1.9
17	0.071±0.008	3.27±0.47	2.4×10^4	3.9
18	0.071±0.008	3.27±0.47	1.1×10^4	1.8
19	10.98±0.21	4.10±0.09	8.6×10^6	9.1
20	34.18±1.28	4.31±0.17	1.0×10^7	3.4
21	4.16±0.15	4.28±0.16	2.6×10^6	7.3
22	0.422±0.014	4.53±0.15	3.2×10^5	8.8
23	0.160±0.010	5.42±0.28	2.6×10^4	1.9
24	0.081±0.007	3.21±0.39	5.6×10^3	0.8
25	0.065±0.003	3.24±0.29	1.5×10^4	2.7
26	0.158±0.017	4.06±0.46	4.5×10^4	3.3

* in particles/m^2-sr-s-MeV/nucleon; ** in particles/m^2-sr-MeV/nucleon.

Table 3: Hydrogen Spectra and SEP Model Parameters

Event	Amplitude A_p*	Index γ_p	Fluence** (at E_0)	Duration (Days)	Fe/O	δ
1	111±8	2.72±0.05	2.88×10^{7}	3	0.155	0.000
2	202±52	3.39±0.18	3.49×10^{7}	2	0.155	0.000
3	37±8	1.94±0.15	6.39×10^{6}	2	0.155	0.000
4	53±9	2.10±0.12	1.83×10^{7}	4	0.306	0.038
5	129±43	3.38±0.24	2.23×10^{7}	2	1.030	0.105
6	56±13	2.38±0.21	4.84×10^{6}	1	1.030	0.105
7	56±8	2.23±0.11	9.68×10^{6}	2	0.226	0.021
8	33±5	1.48±0.11	2.85×10^{6}	1	1.030	0.105
9	75±13	2.40±0.12	6.48×10^{6}	1	1.030	0.105
10	20040±7001	4.64±0.40	3.46×10^{9}	2	0.946	0.101
11	579±115	4.16±0.23	2.00×10^{8}	4	5.243	0.196
12	91±11	2.70±0.08	1.57×10^{7}	2	0.155	0.000
13	31±5	1.45±0.11	2.68×10^{6}	1	1.030	0.105
14	30±4	1.40±0.09	2.59×10^{6}	1	1.030	0.105
15	50±4	1.97±0.05	4.32×10^{6}	1	1.030	0.105
16	445±66	3.08±0.13	7.69×10^{7}	2	6.208	0.205
17	71±6	2.25±0.06	2.45×10^{7}	4	0.155	0.000
18	83±12	2.74±0.11	1.43×10^{7}	2	0.155	0.000
19	876±140	3.08±0.19	6.81×10^{8}	9	0.102	-0.023
20	3238±917	2.90±0.26	1.12×10^{9}	4	0.059	-0.054
21	1261±307	2.76±0.22	8.72×10^{8}	8	0.492	0.064
22	153±23	2.84±0.11	1.19×10^{8}	9	0.155	0.000
23	306±119	4.10±0.28	7.93×10^{7}	3	1.030	0.105
24	24±4	1.38±0.11	2.07×10^{6}	1	1.030	0.105
25	131±34	3.26±0.18	4.53×10^{7}	4	0.155	0.000
26	71±10	2.45±0.10	2.45×10^{7}	4	9.336	0.228

* in particles/m^2-sr-s-MeV/nucleon; ** in particles/m^2-sr-MeV/nucleon.

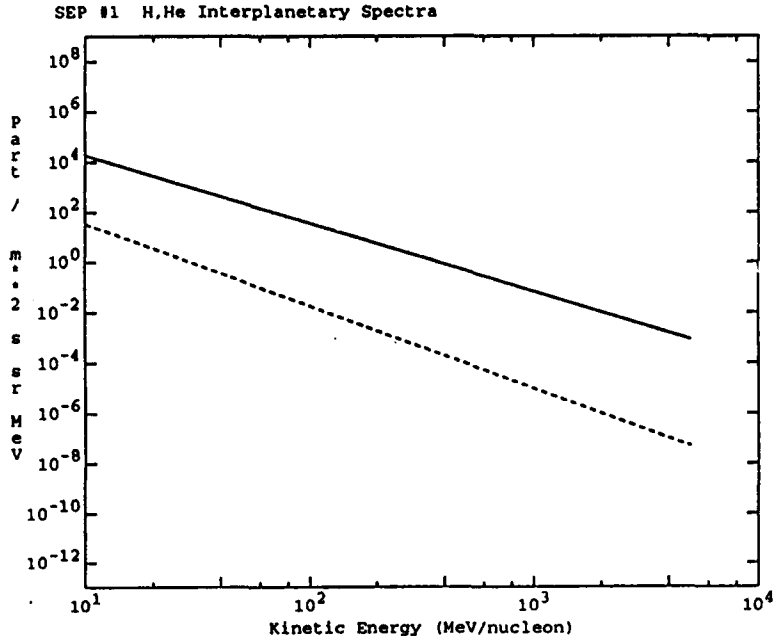
SEP #1 H,He Interplanetary Spectra
part / m**2 s sr MeV
Kinetic Energy (MeV/nucleon)

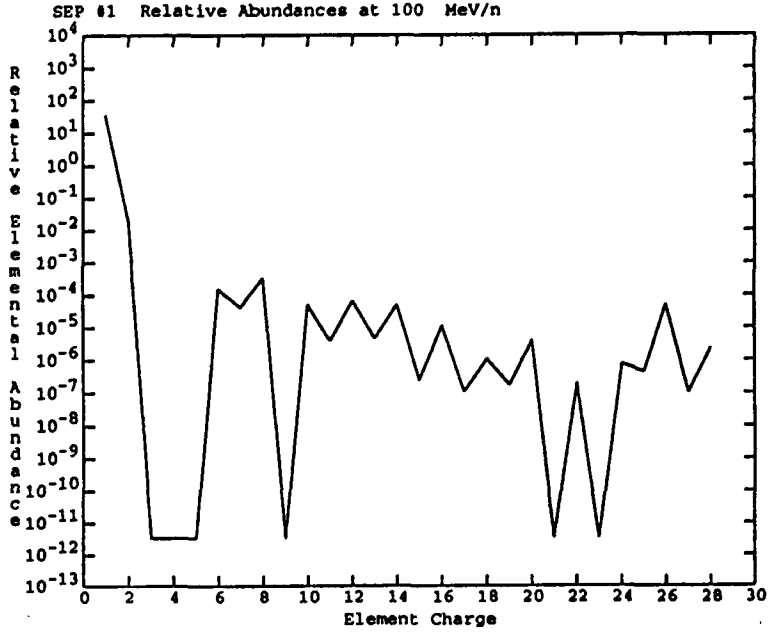
SEP #1 Relative Abundances at 100 MeV/n
Relative Elemental Abundance
Element Charge

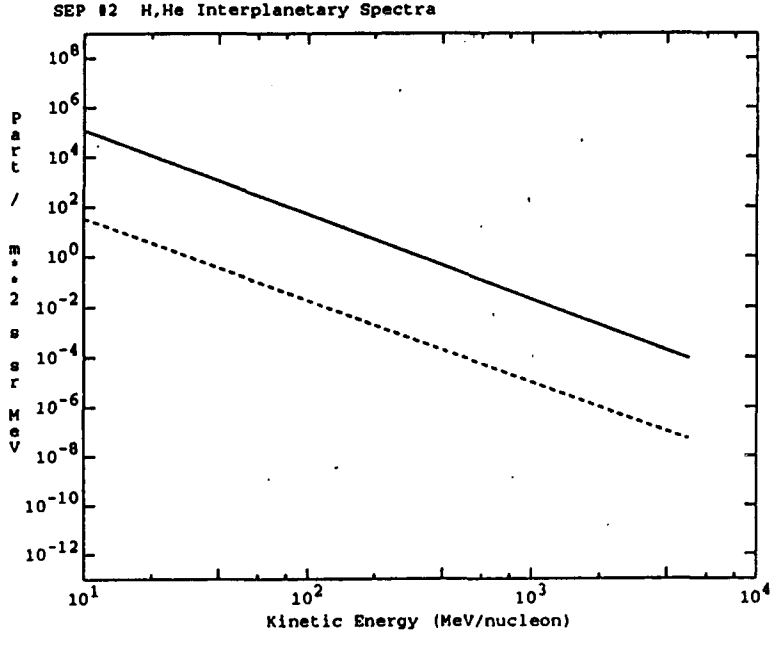
SEP #2 H,He Interplanetary Spectra
part / m**2 s sr MeV
Kinetic Energy (MeV/nucleon)

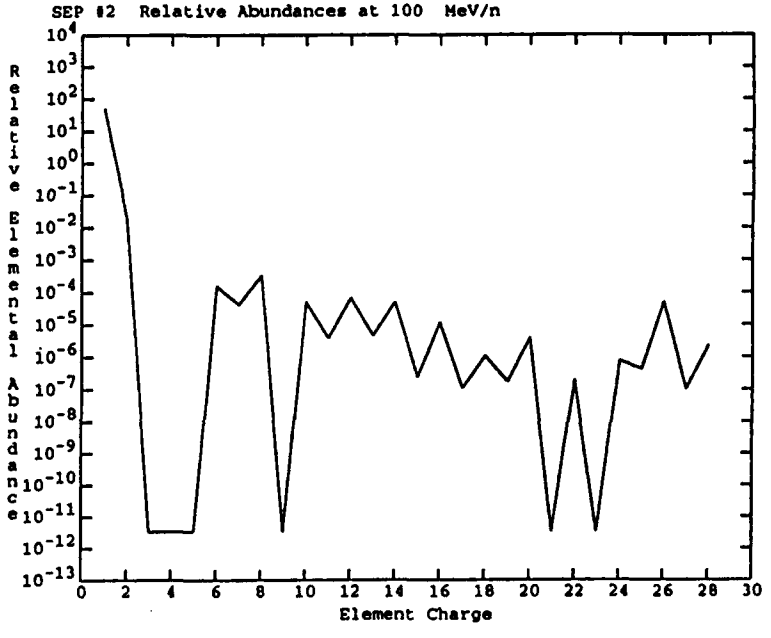
SEP #2 Relative Abundances at 100 MeV/n
Relative Elemental Abundance
Element Charge

FIGURE 2 a

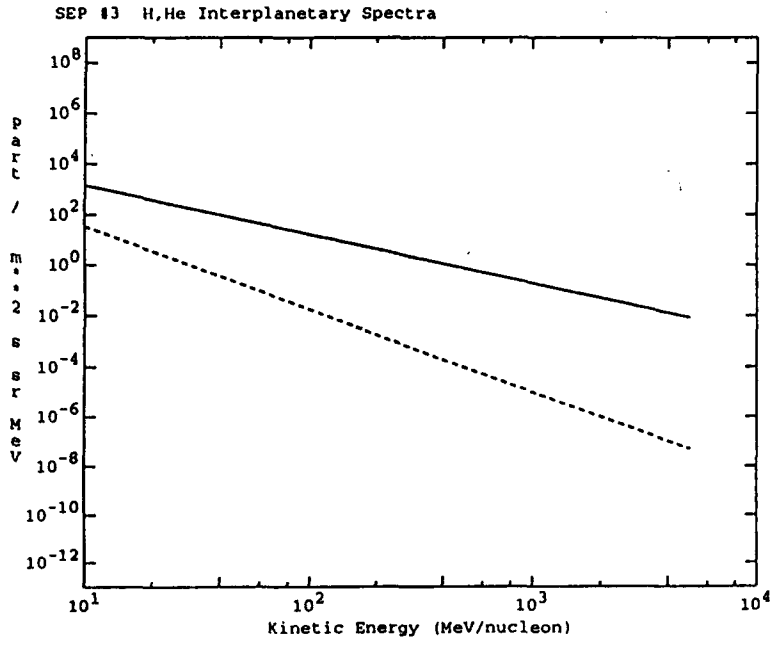
SEP #3 H,He Interplanetary Spectra
part / m**2 s sr MeV
Kinetic Energy (MeV/nucleon)

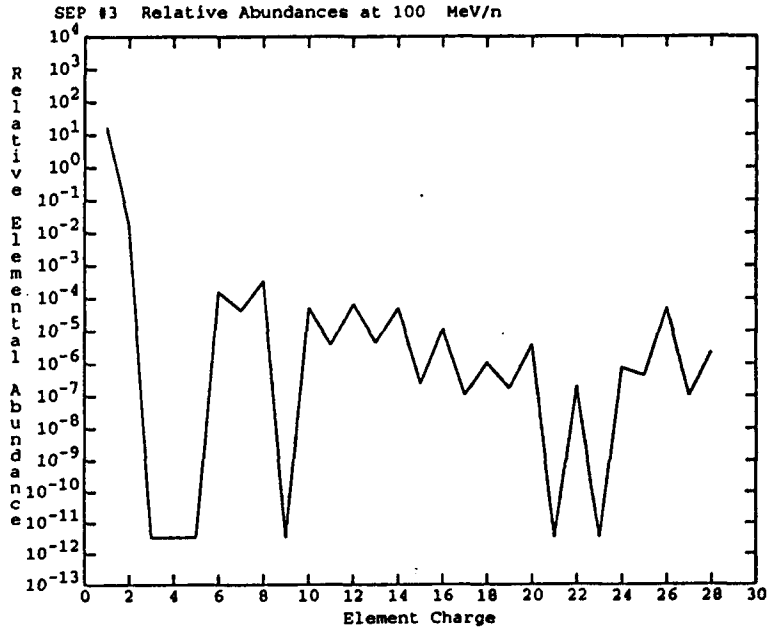
SEP #3 Relative Abundances at 100 MeV/n
Relative Elemental Abundance
Element Charge

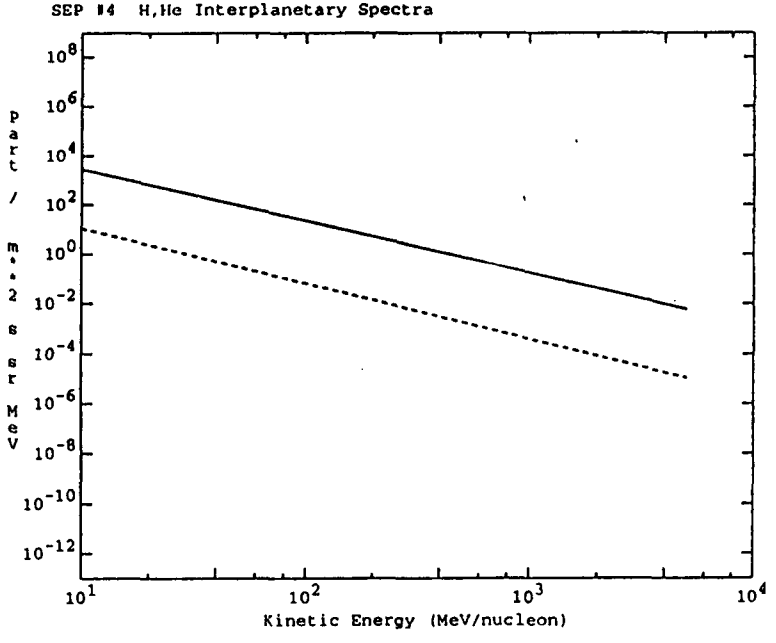
SEP #4 H,He Interplanetary Spectra
part / m**2 s sr MeV
Kinetic Energy (MeV/nucleon)

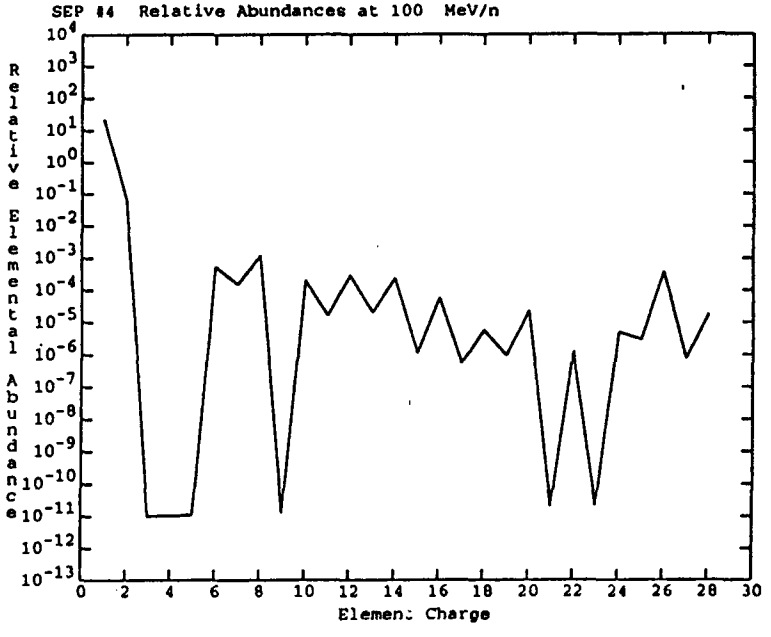
SEP #4 Relative Abundances at 100 MeV/n
Relative Elemental Abundance
Element Charge

FIGURE 2b

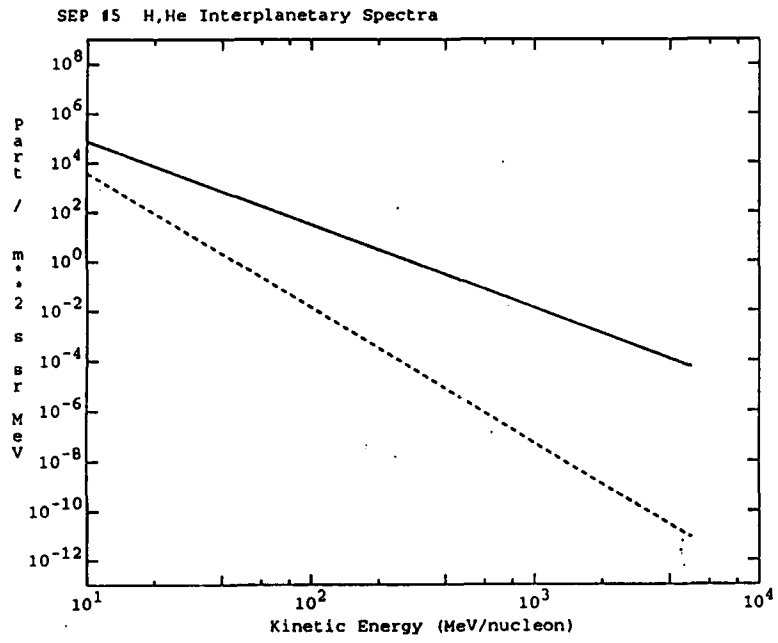
SEP #5 H,He Interplanetary Spectra
Part / m**2 s sr MeV
Kinetic Energy (MeV/nucleon)

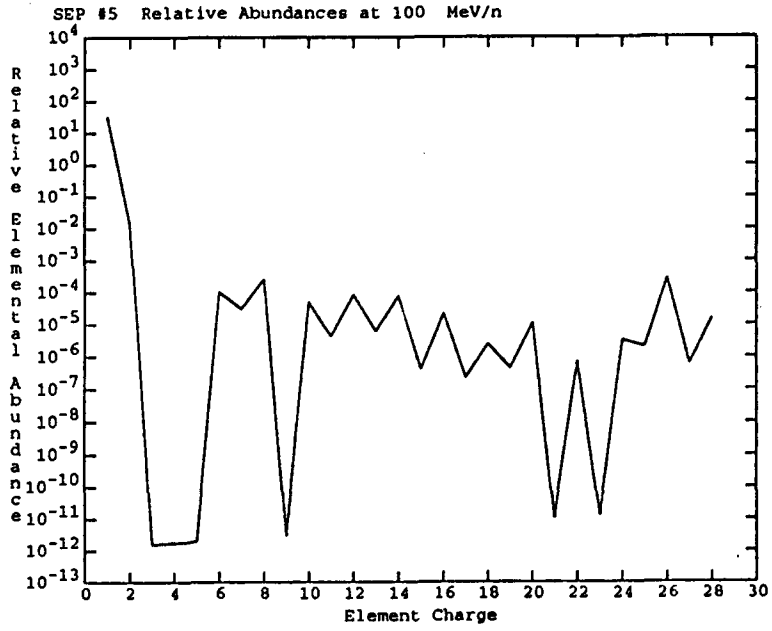
SEP #5 Relative Abundances at 100 MeV/n
Relative Elemental Abundance
Element Charge

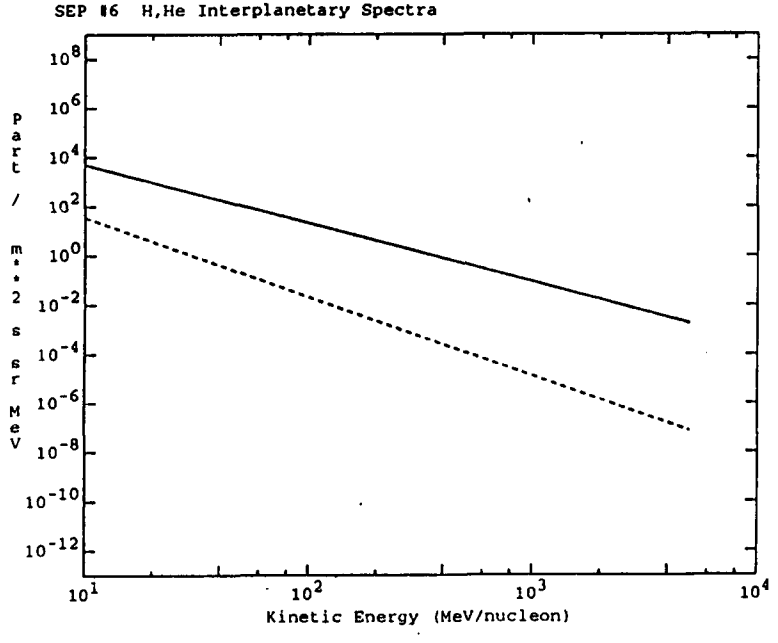
SEP #6 H,He Interplanetary Spectra
Part / m**2 s sr MeV
Kinetic Energy (MeV/nucleon)

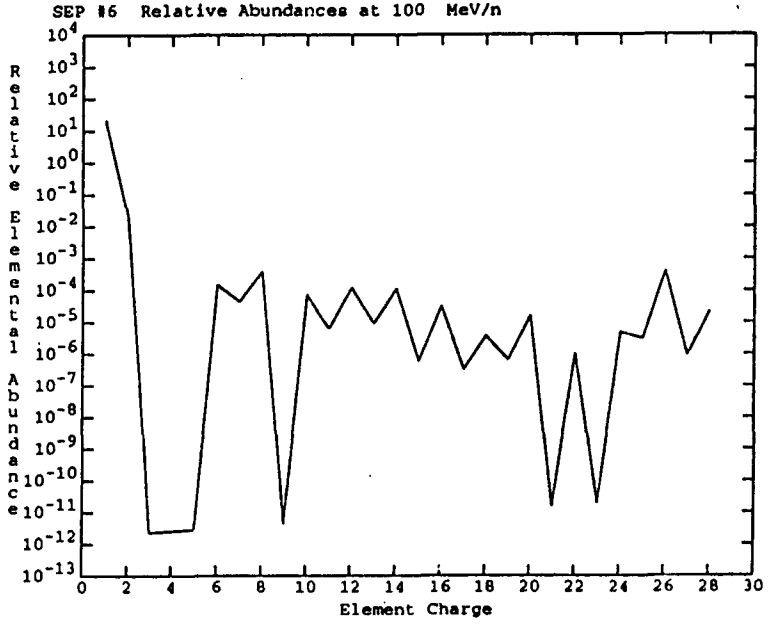
SEP #6 Relative Abundances at 100 MeV/n
Relative Elemental Abundance
Element Charge

FIGURE 2c

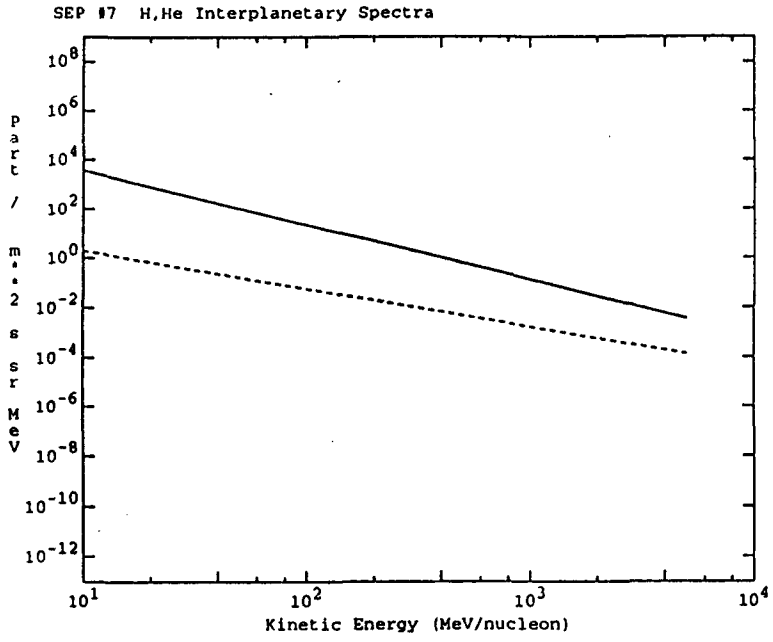
SEP #7 H,He Interplanetary Spectra
part / m**2 s sr MeV
Kinetic Energy (MeV/nucleon)

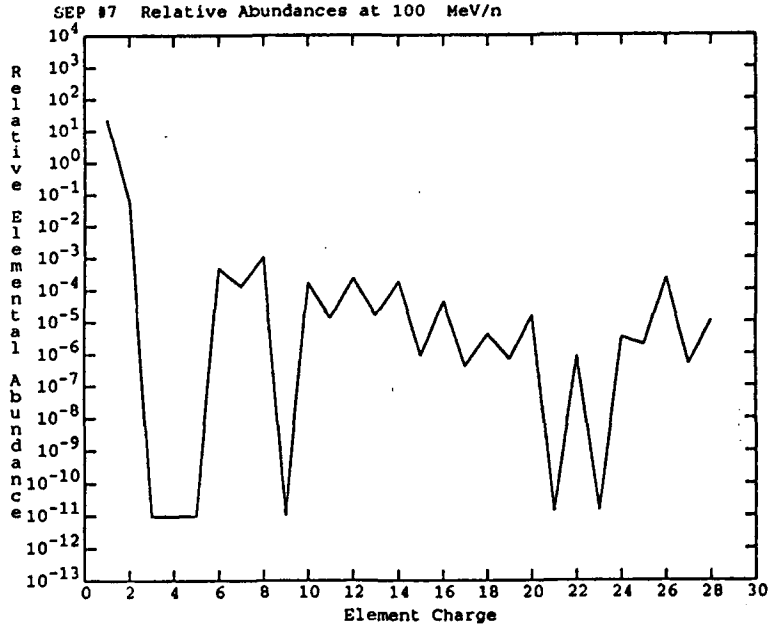
SEP #7 Relative Abundances at 100 MeV/n
Relative Elemental Abundance
Element Charge

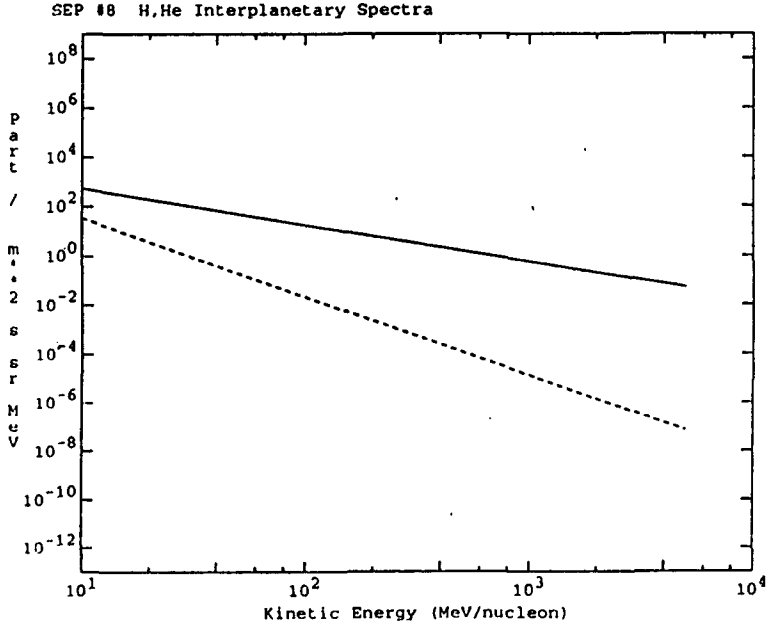
SEP #8 H,He Interplanetary Spectra
part / m**2 s sr MeV
Kinetic Energy (MeV/nucleon)

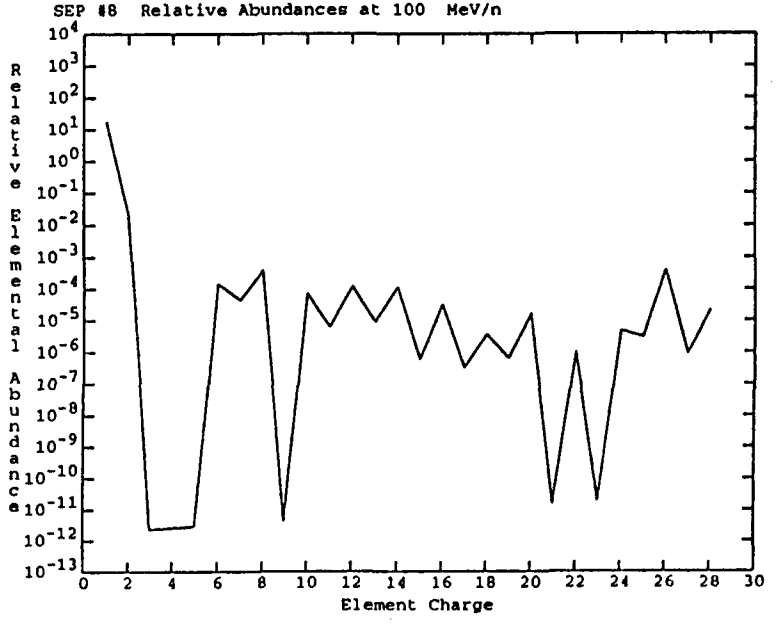
SEP #8 Relative Abundances at 100 MeV/n
Relative Elemental Abundance
Element Charge

FIGURE 2d

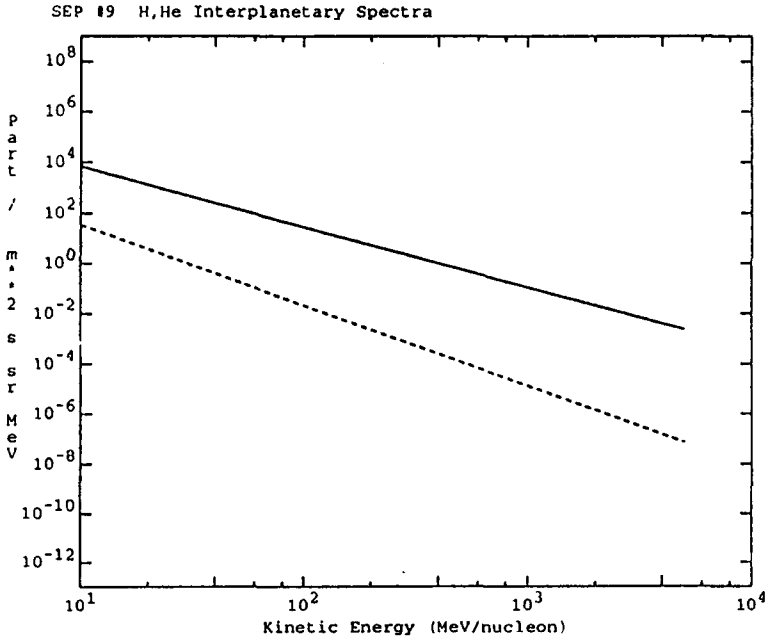
SEP #9 H,He Interplanetary Spectra
part / m**2 s sr MeV
Kinetic Energy (MeV/nucleon)

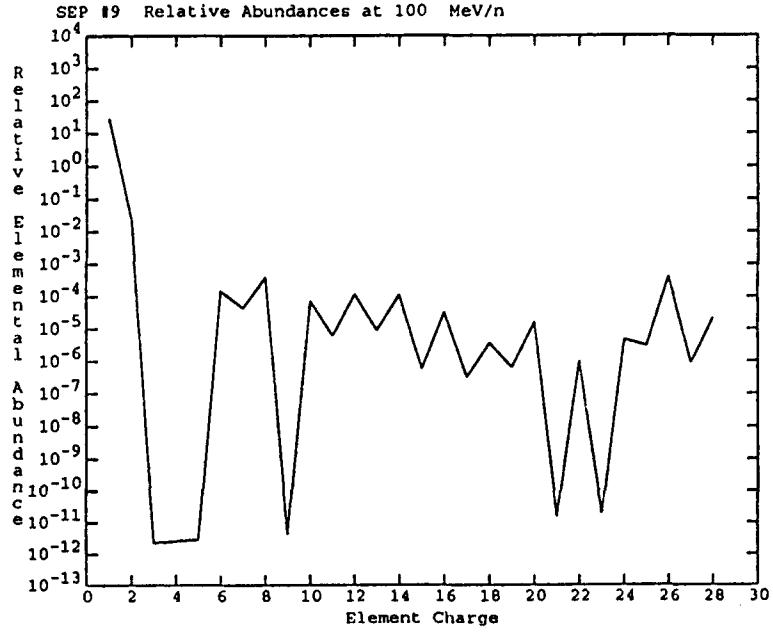
SEP #9 Relative Abundances at 100 MeV/n
Relative Elemental Abundance
Element Charge

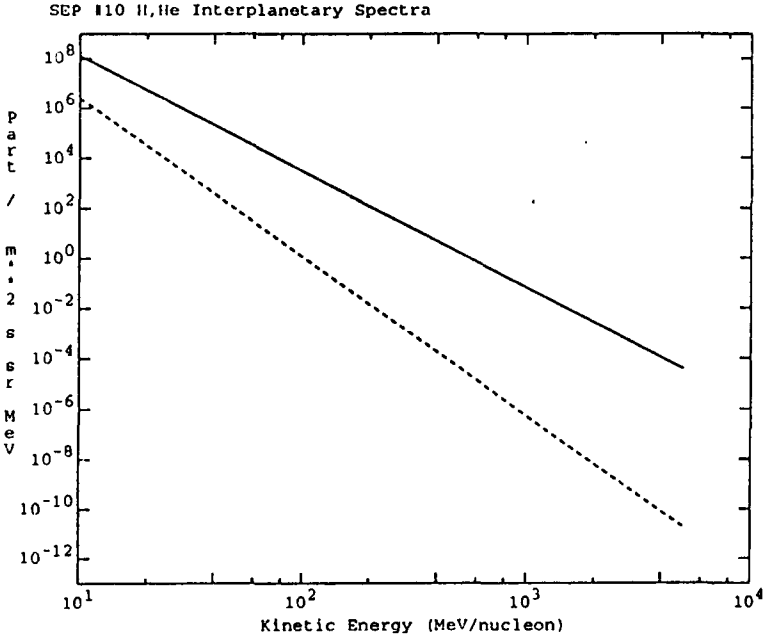
SEP #10 H,He Interplanetary Spectra
part / m**2 s sr MeV
Kinetic Energy (MeV/nucleon)

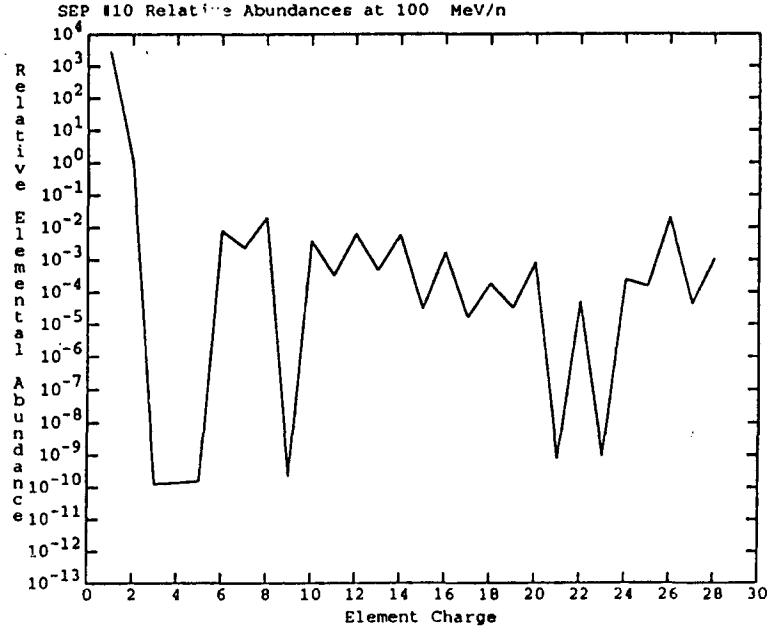
SEP #10 Relative Abundances at 100 MeV/n
Relative Elemental Abundance
Element Charge

FIGURE 2e

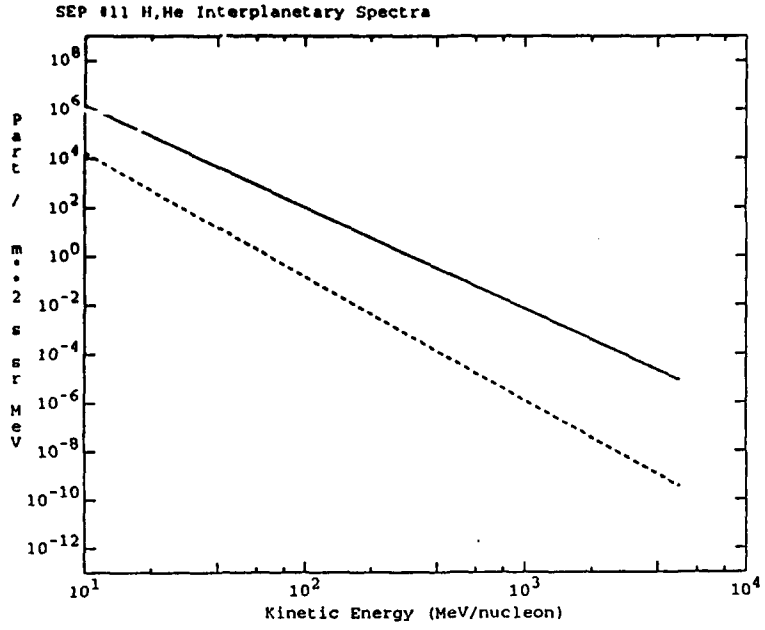
SEP #11 H,He Interplanetary Spectra
part / m**2 s sr MeV
Kinetic Energy (MeV/nucleon)

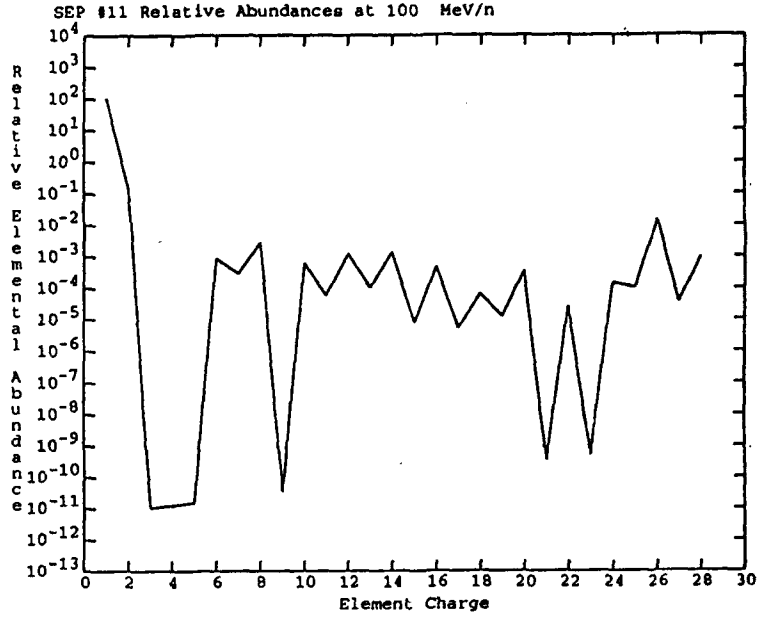
SEP #11 Relative Abundances at 100 MeV/n
Relative Elemental Abundance
Element Charge

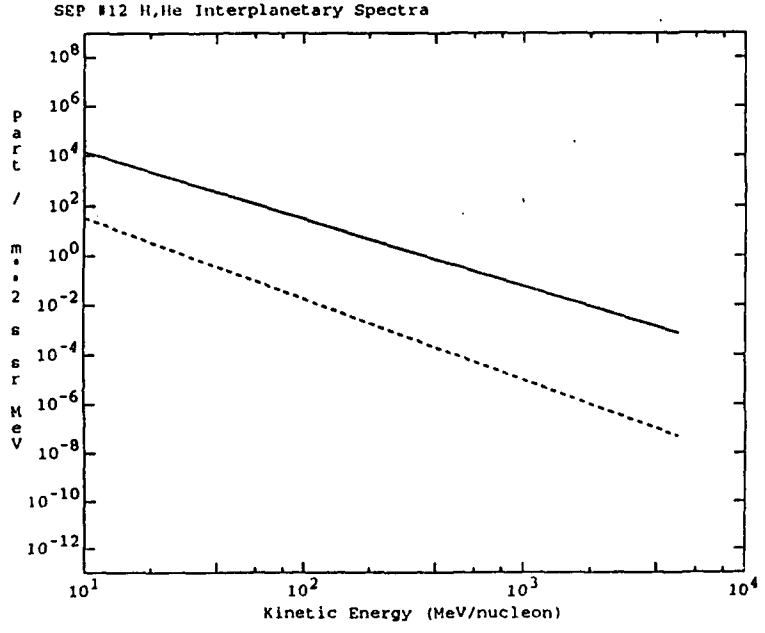
SEP #12 H,He Interplanetary Spectra
part / m**2 s sr MeV
Kinetic Energy (MeV/nucleon)

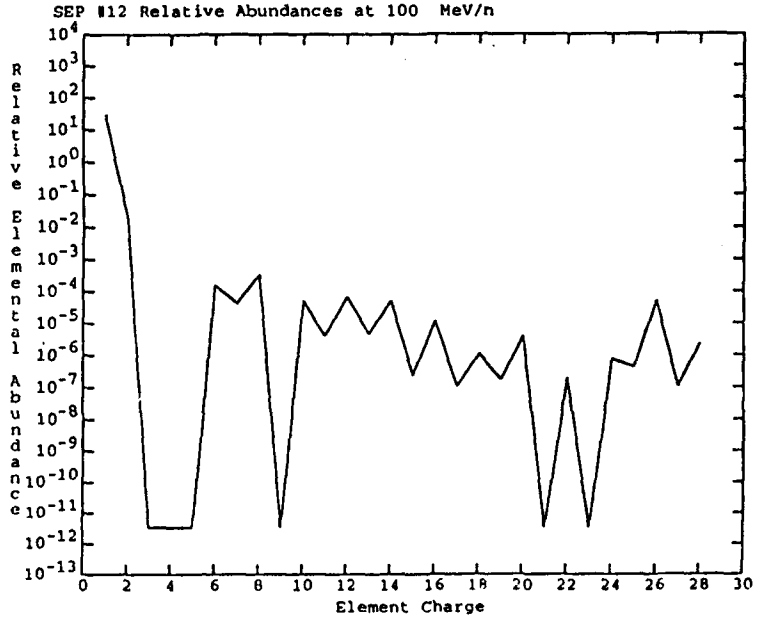
SEP #12 Relative Abundances at 100 MeV/n
Relative Elemental Abundance
Element Charge

FIGURE 2f

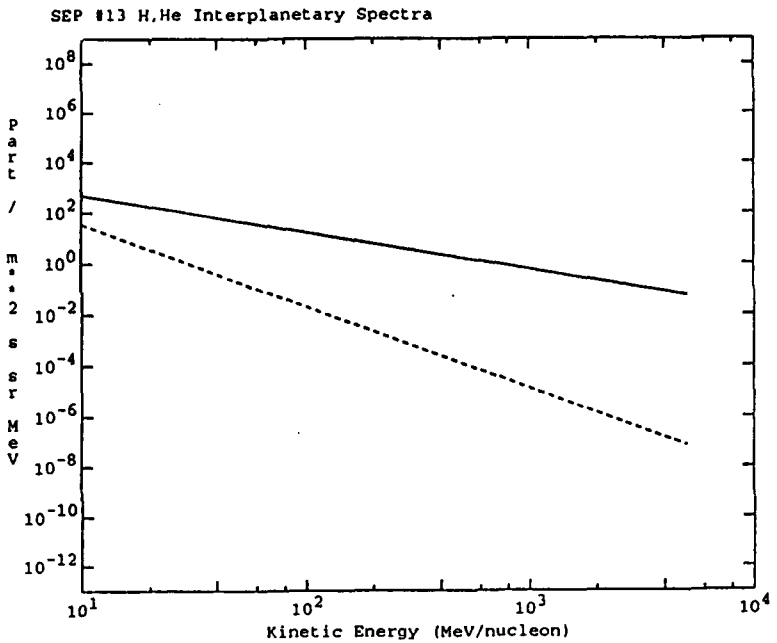
SEP #13 H,He Interplanetary Spectra
part / m**2 s sr MeV
Kinetic Energy (MeV/nucleon)

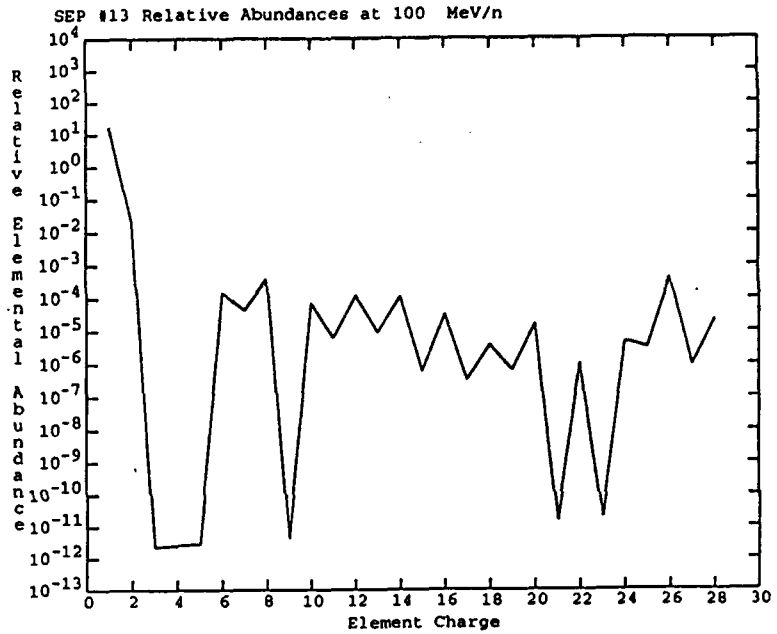
SEP #13 Relative Abundances at 100 MeV/n
Relative Elemental Abundance
Element Charge

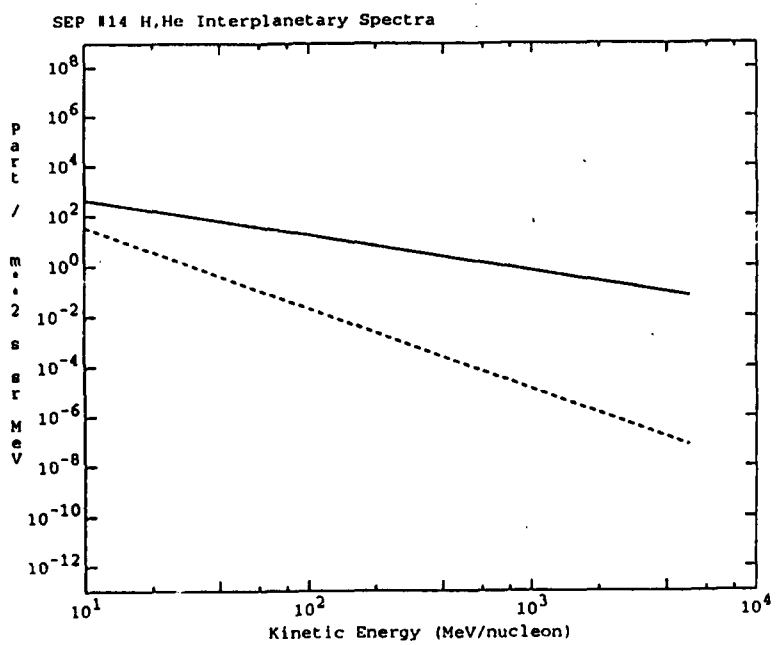
SEP #14 H,He Interplanetary Spectra
part / m**2 s sr MeV
Kinetic Energy (MeV/nucleon)

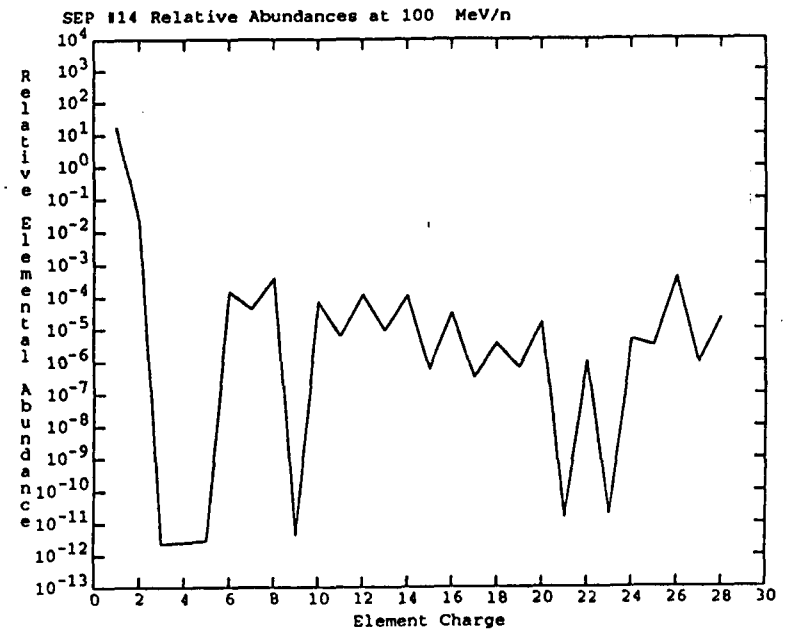
SEP #14 Relative Abundances at 100 MeV/n
Relative Elemental Abundance
Element Charge

FIGURE 2g

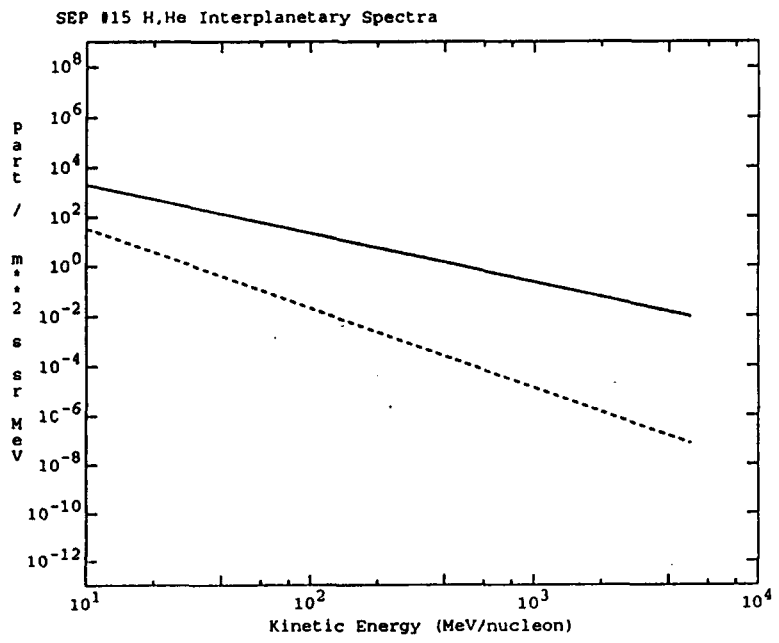
SEP #15 H,He Interplanetary Spectra
part / m**2 s sr MeV
Kinetic Energy (MeV/nucleon)

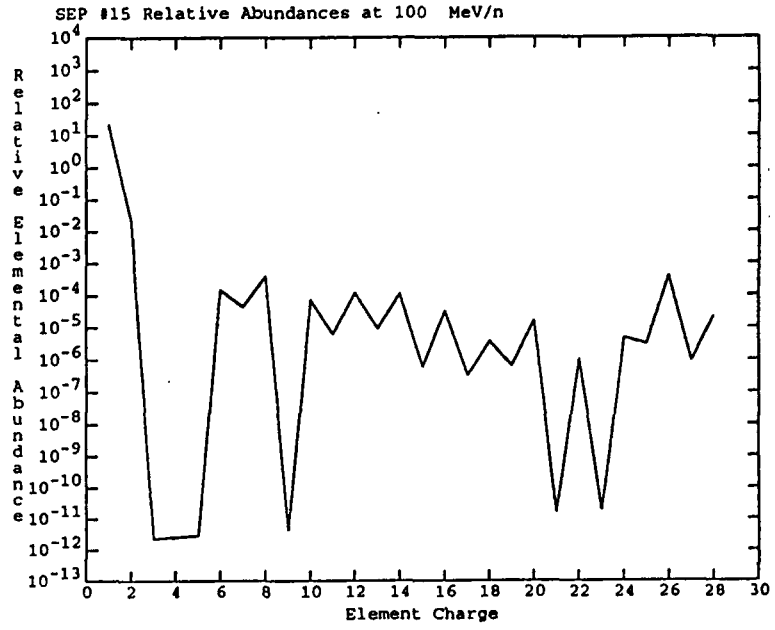
SEP #15 Relative Abundances at 100 MeV/n
Relative Elemental Abundance
Element Charge

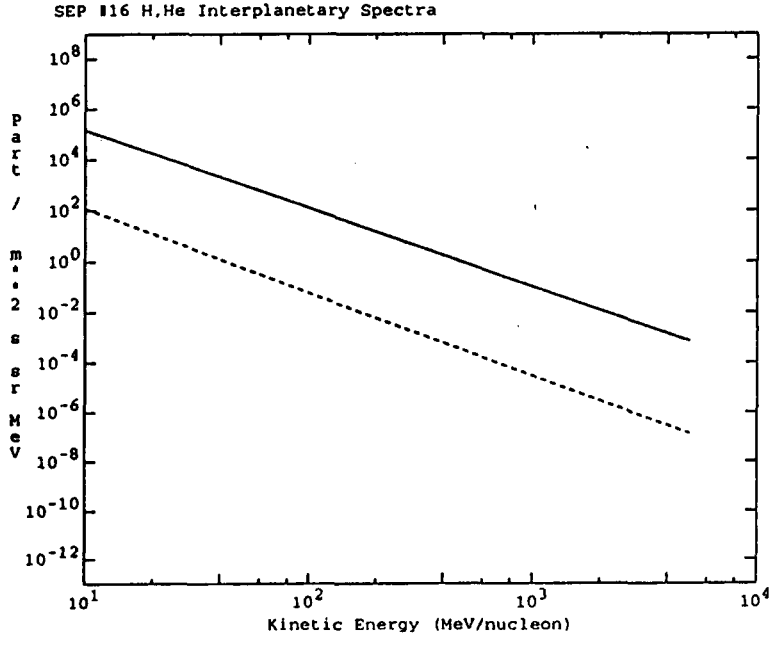
SEP #16 H,He Interplanetary Spectra
part / m**2 s sr MeV
Kinetic Energy (MeV/nucleon)

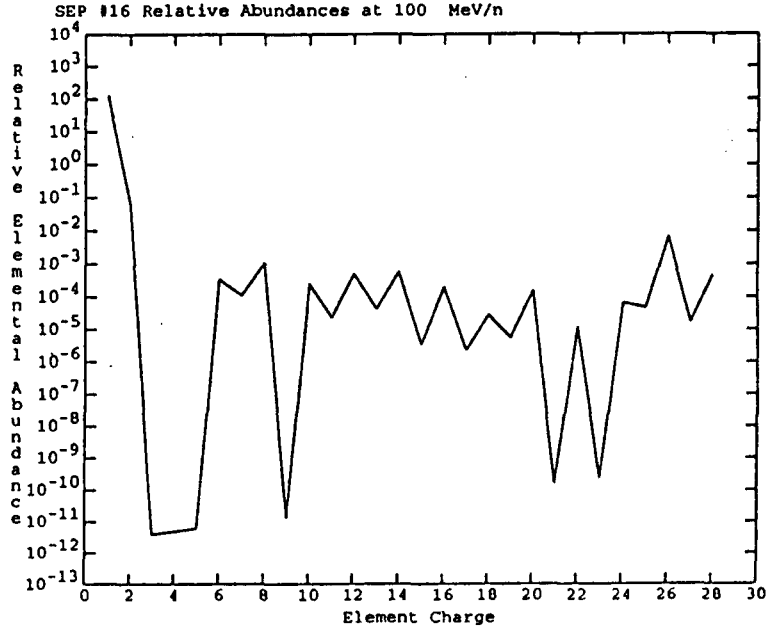
SEP #16 Relative Abundances at 100 MeV/n
Relative Elemental Abundance
Element Charge

FIGURE 2h

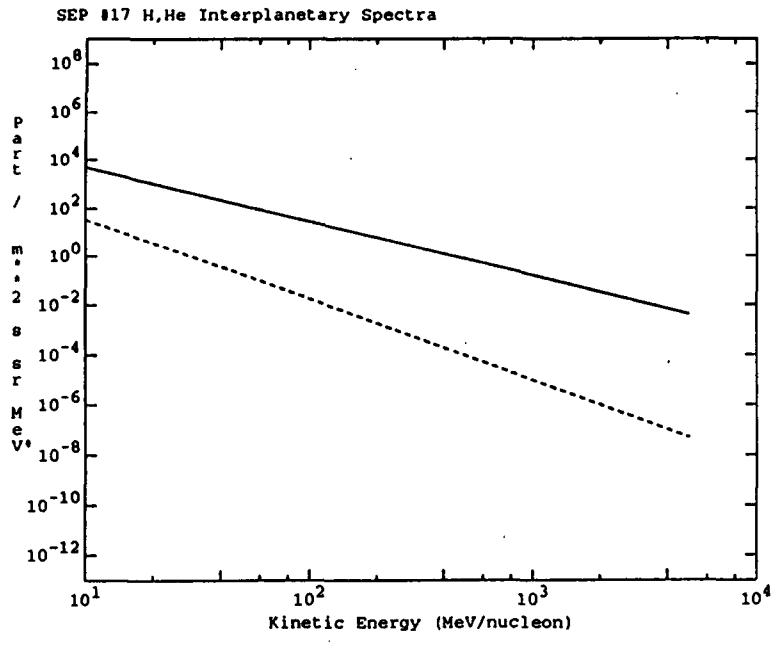
SEP #17 H,He Interplanetary Spectra
Part / m^2 s sr MeV*
Kinetic Energy (MeV/nucleon)

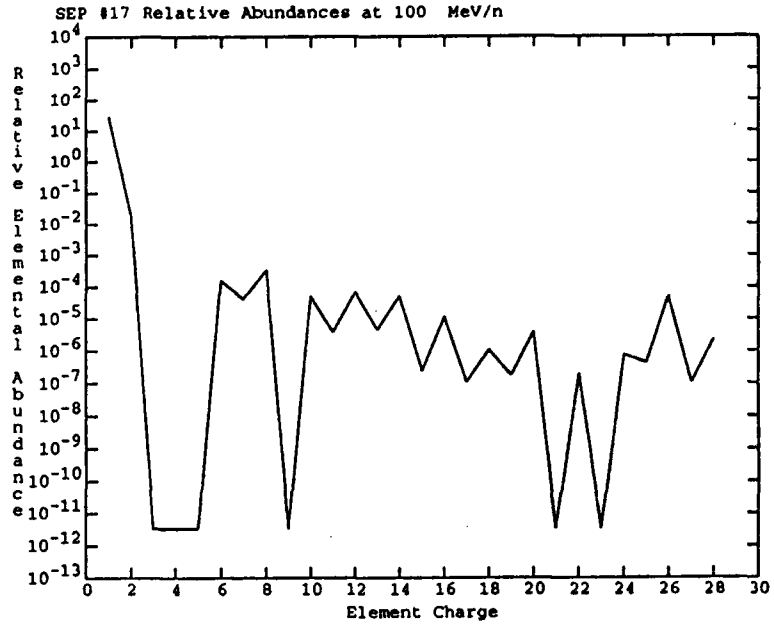
SEP #17 Relative Abundances at 100 MeV/n
Relative Elemental Abundance
Element Charge

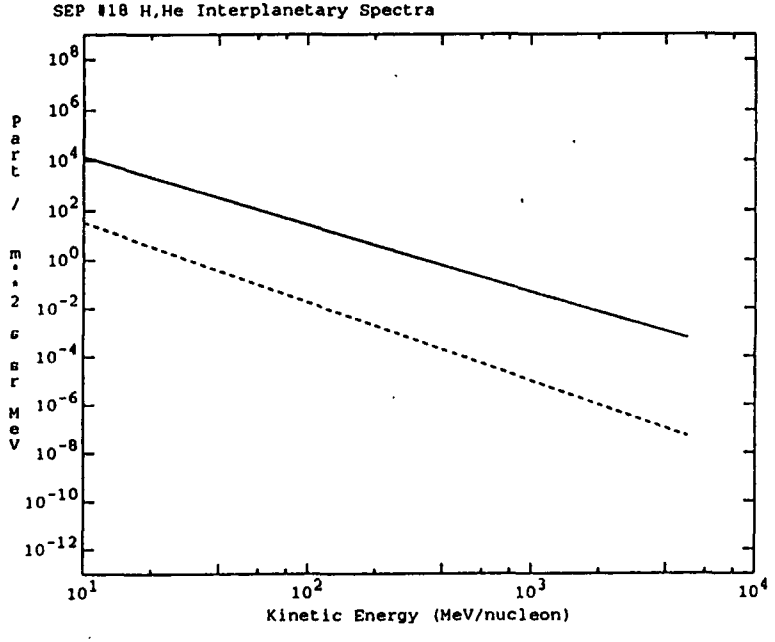
SEP #18 H,He Interplanetary Spectra
Part / m^2 s sr MeV
Kinetic Energy (MeV/nucleon)

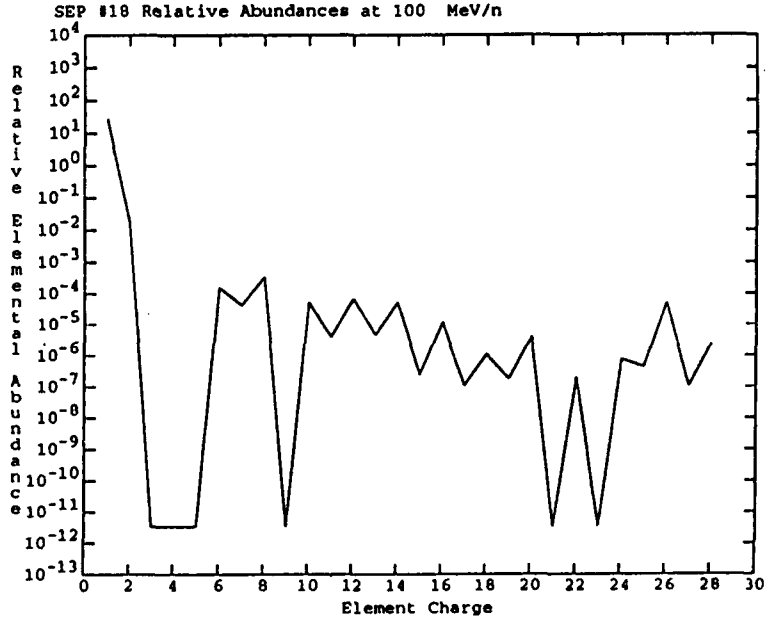
SEP #18 Relative Abundances at 100 MeV/n
Relative Elemental Abundance
Element Charge

FIGURE 2i

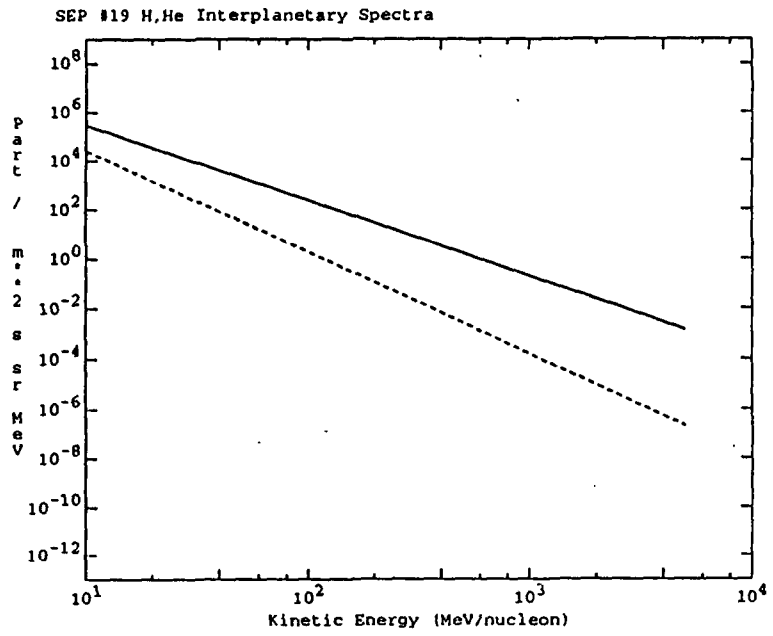
SEP #19 H,He Interplanetary Spectra
part / m**2 sr MeV
Kinetic Energy (MeV/nucleon)

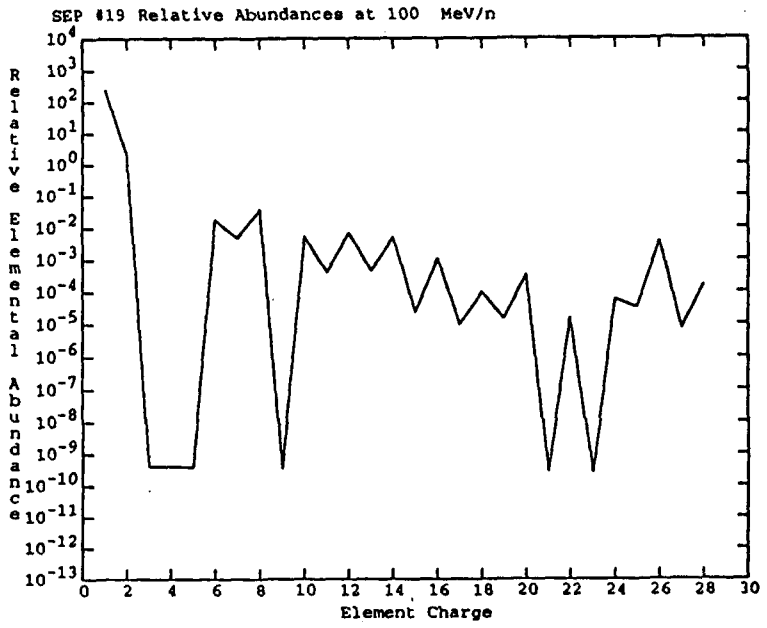
SEP #19 Relative Abundances at 100 MeV/n
Relative Elemental Abundance
Element Charge

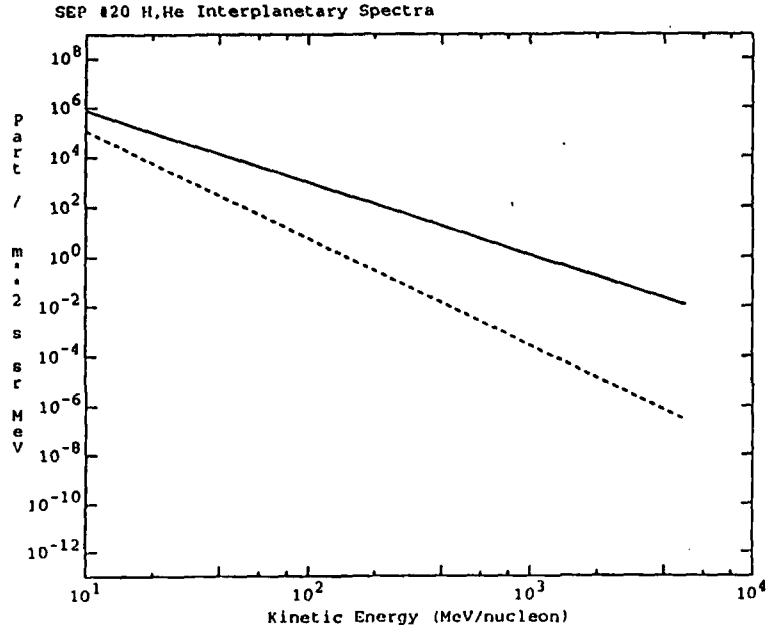
SEP #20 H,He Interplanetary Spectra
part / m**2 sr MeV
Kinetic Energy (MeV/nucleon)

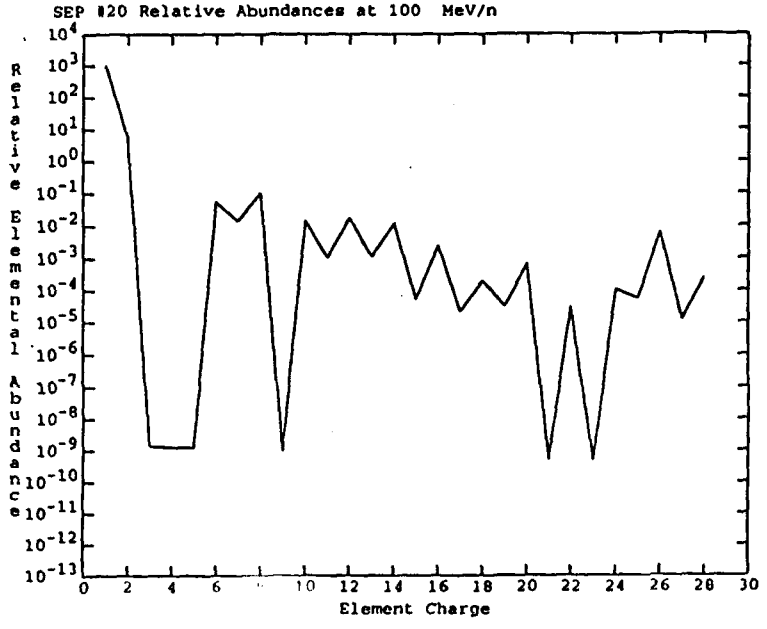
SEP #20 Relative Abundances at 100 MeV/n
Relative Elemental Abundance
Element Charge

FIGURE 2j

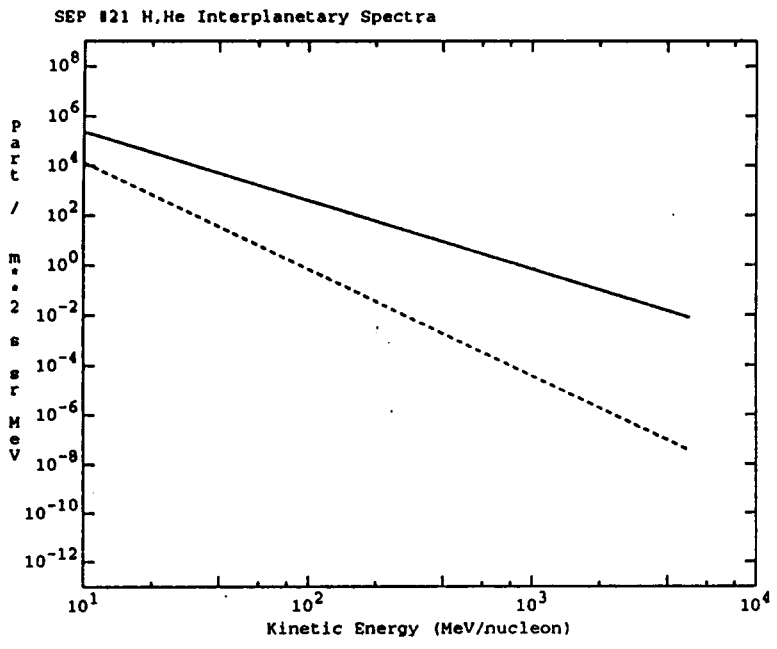
SEP #21 H,He Interplanetary Spectra
part / m**2 sr MeV
Kinetic Energy (MeV/nucleon)

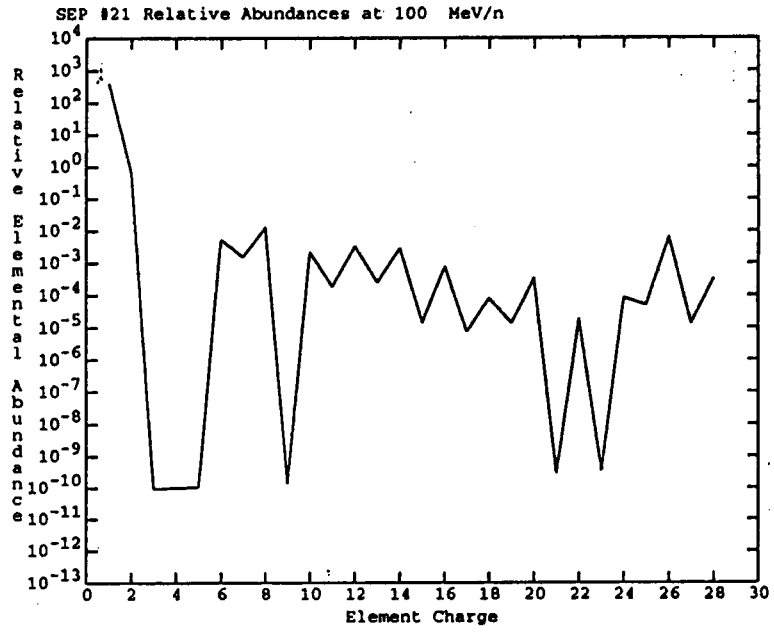
SEP #21 Relative Abundances at 100 MeV/n
Relative Elemental Abundance
Element Charge

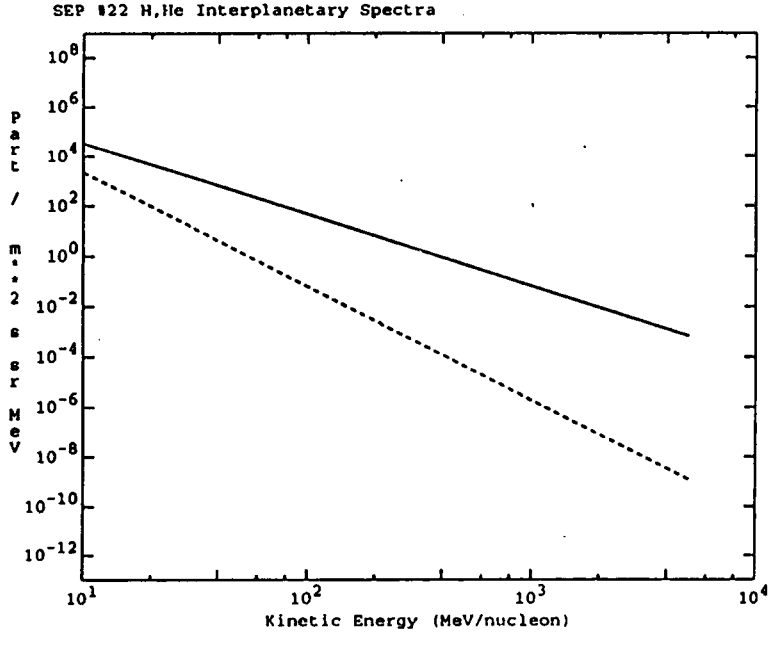
SEP #22 H,He Interplanetary Spectra
part / m**2 sr MeV
Kinetic Energy (MeV/nucleon)

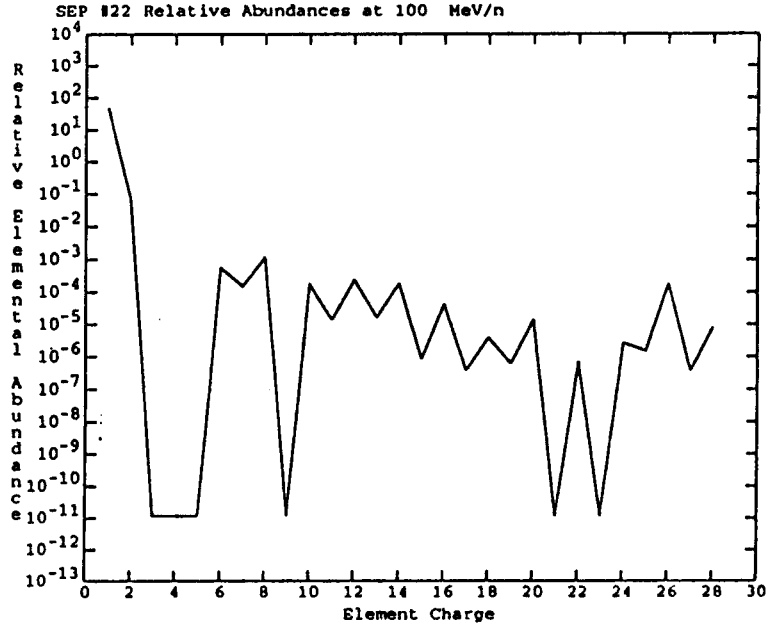
SEP #22 Relative Abundances at 100 MeV/n
Relative Elemental Abundance
Element Charge

FIGURE 2k

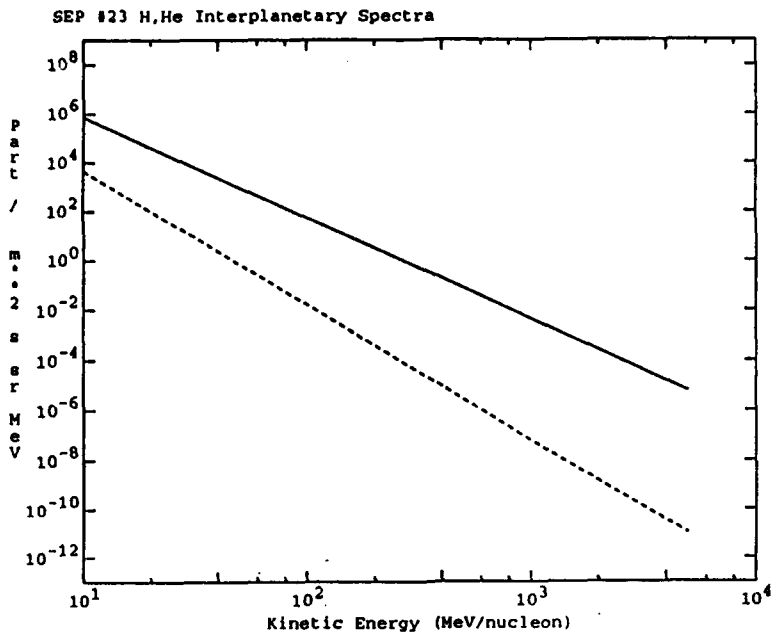
SEP #23 H,He Interplanetary Spectra
part / m**2 sr MeV
Kinetic Energy (MeV/nucleon)

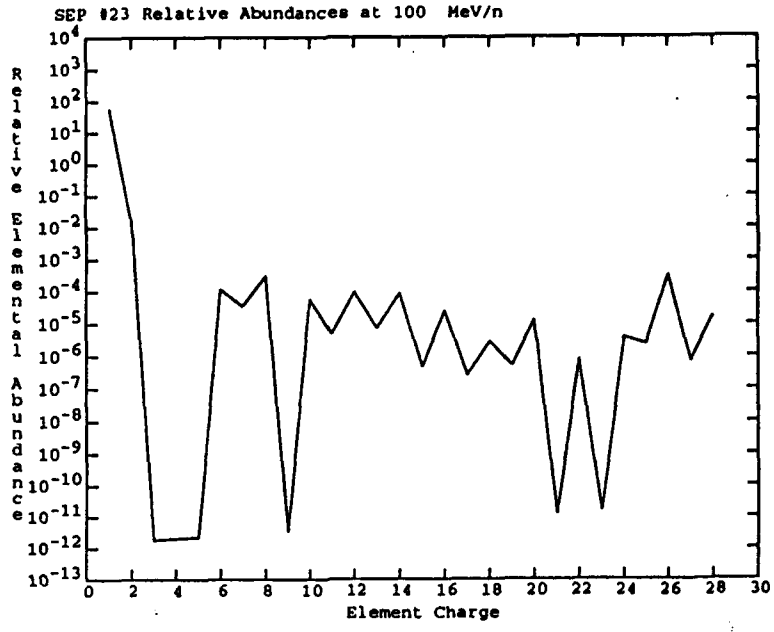
SEP #23 Relative Abundances at 100 MeV/n
Relative Elemental Abundance
Element Charge

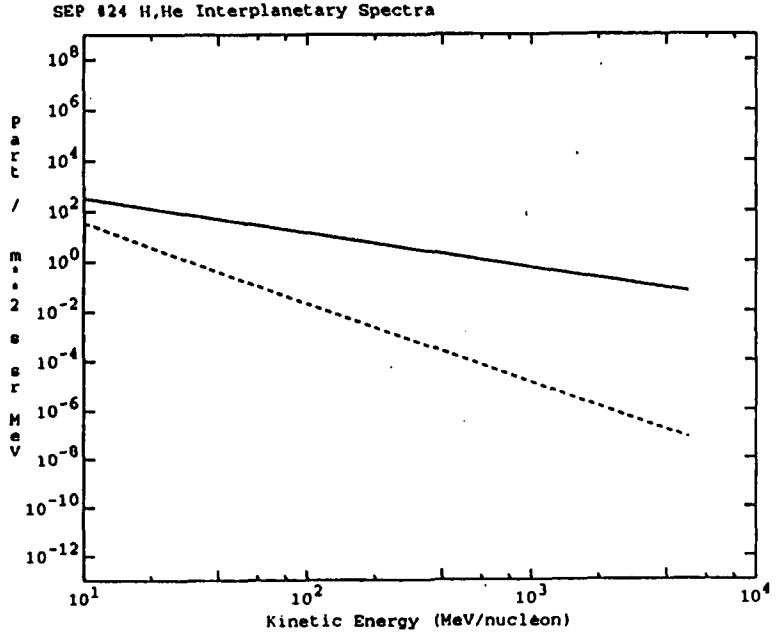
SEP #24 H,He Interplanetary Spectra
part / m**2 sr MeV
Kinetic Energy (MeV/nucleon)

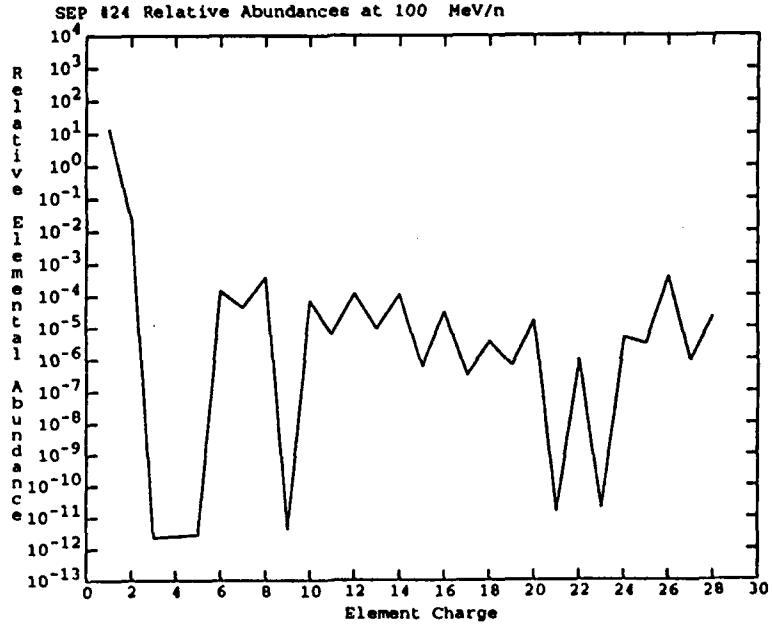
SEP #24 Relative Abundances at 100 MeV/n
Relative Elemental Abundance
Element Charge

FIGURE 21

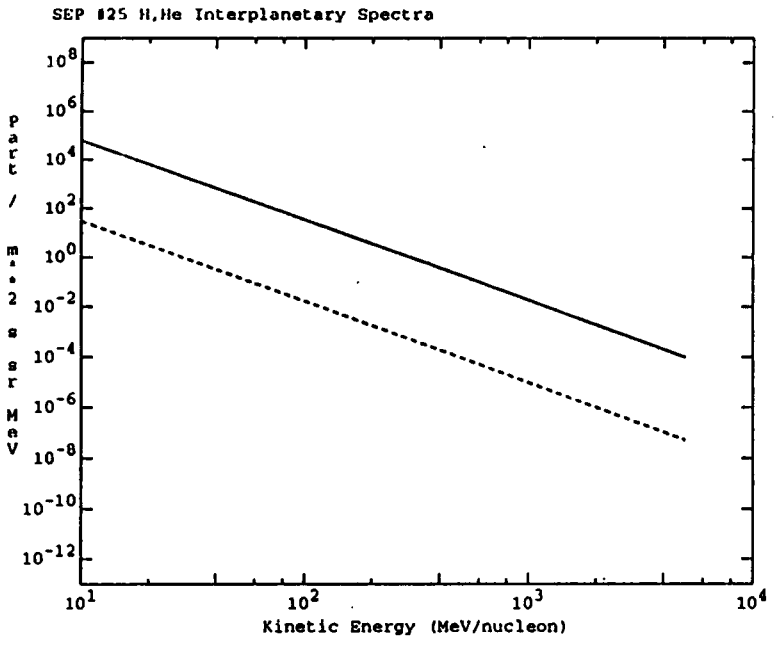
SEP #25 H,He Interplanetary Spectra
Part / m**2 s sr MeV
Kinetic Energy (MeV/nucleon)

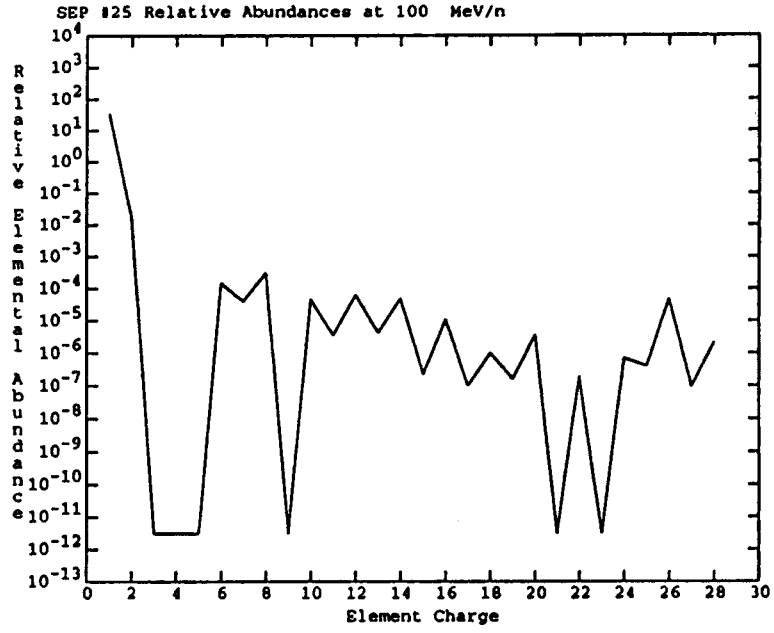
SEP #25 Relative Abundances at 100 MeV/n
Relative Elemental Abundance
Element Charge

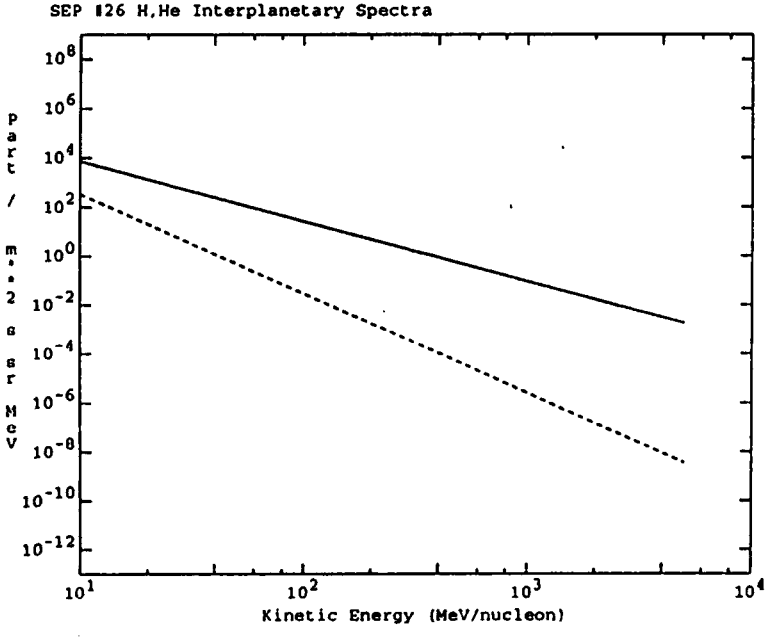
SEP #26 H,He Interplanetary Spectra
Part / m**2 s sr MeV
Kinetic Energy (MeV/nucleon)

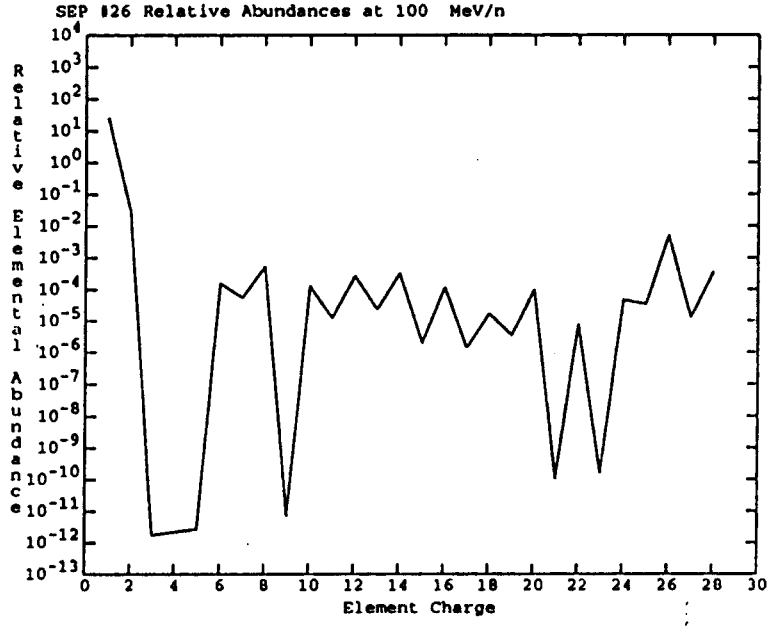
SEP #26 Relative Abundances at 100 MeV/n
Relative Elemental Abundance
Element Charge

FIGURE 2 m

For the future we plan to focus upon producing a manuscript on the larger flares for publication. In addition, it would be valuable to be able to predict for a future time what a probable flare environment might be, at least on yearly time-scales. This should be possible with the accumulated SEP data from many satellites, normalized to the ONR-604 results presented here. Such a study will be one of our tasks for the coming periods.

III. GCR Energy Spectra

Working with the University of Chicago group, one of our tasks has been to compare predictions of the GCR flux and energy spectra to the actual observations made by the ONR-604 instrument. This is not as simple a job as it seems, since the ONR-604 system encompasses three priority ranges (P1, P2 and P3) and has a very wide field-of-view.

The first results of such a comparison are shown in Figure 3 for helium and Figure 4 for oxygen. The ONR-604 data are represented as crosses to be compared to the solid lines which are the predictions. These predictions result from using a best fit to the local interstellar energy spectrum of each element and modulating that spectrum to Earth using a modulation parameter, phi, of 1455 MV, the best average value for the overall CRRES mission. Also shown for comparison is available IMP-8 data; the 70-95 MeV/nucleon helium flux for the CRRES period in Figure 3 and the oxygen energy spectrum for August 90 to March 91 in Figure 4, which covers the first part of the CRRES mission. Note that the ONR-604 data fall consistently below both the predictions and the IMP-8 results. Relative to the predictions, the ONR-604 results are low by ~20%. Plots for other elements, e.g. silicon or iron, show the same trend with the data ~20% below the predictions.

It is possible that the predictions are somehow in error, although Figure 4 argues against this. As a further check, we have gone back to an independent solar minimum, IMP-8, oxygen spectrum prepared by the University of Chicago some years ago. The comparison of this spectrum with the predictions, Figure 5, shows excellent agreement. Thus, we believe that the disagreement is not due to the predictions but rather to the normalization of the ONR-604 dataset.

The fact that the ONR-604 flux values are ~80% of the predictions for <u>both</u> P1 and P2 events, independent of charge from He-Fe, indicates a systematic effect. Both P1 and P2 analysis requires a clean event, i.e. one in which the scintillator, S, did not fire. If S is noisy, or there is a large radiation background outside the instrument that triggers S at a large rate, or some events near the edges of the detectors eject a particle (proton or electron) that penetrates to S, the observations could be explained. We are investigating these possibilities by using data only from radiation quiet portions of the orbit, by using the trajectory system to remove events that are near the detector edges (requiring a re-calculation of the geometric factors) and by examining the S firing rate as a function of time. Preliminary results show that these changes (taken together) increase the calculated flux values by 15-20%, bringing the ONR-604 results into better agreement with IMP-8 results and with the predictions.

The importance of this analysis lies in the information it supplies about the operation of the ONR-604 instrument. We are already re-doing some of our previous analyses to take into account the edge effects and other parameters. These will be discussed in subsequent reports.

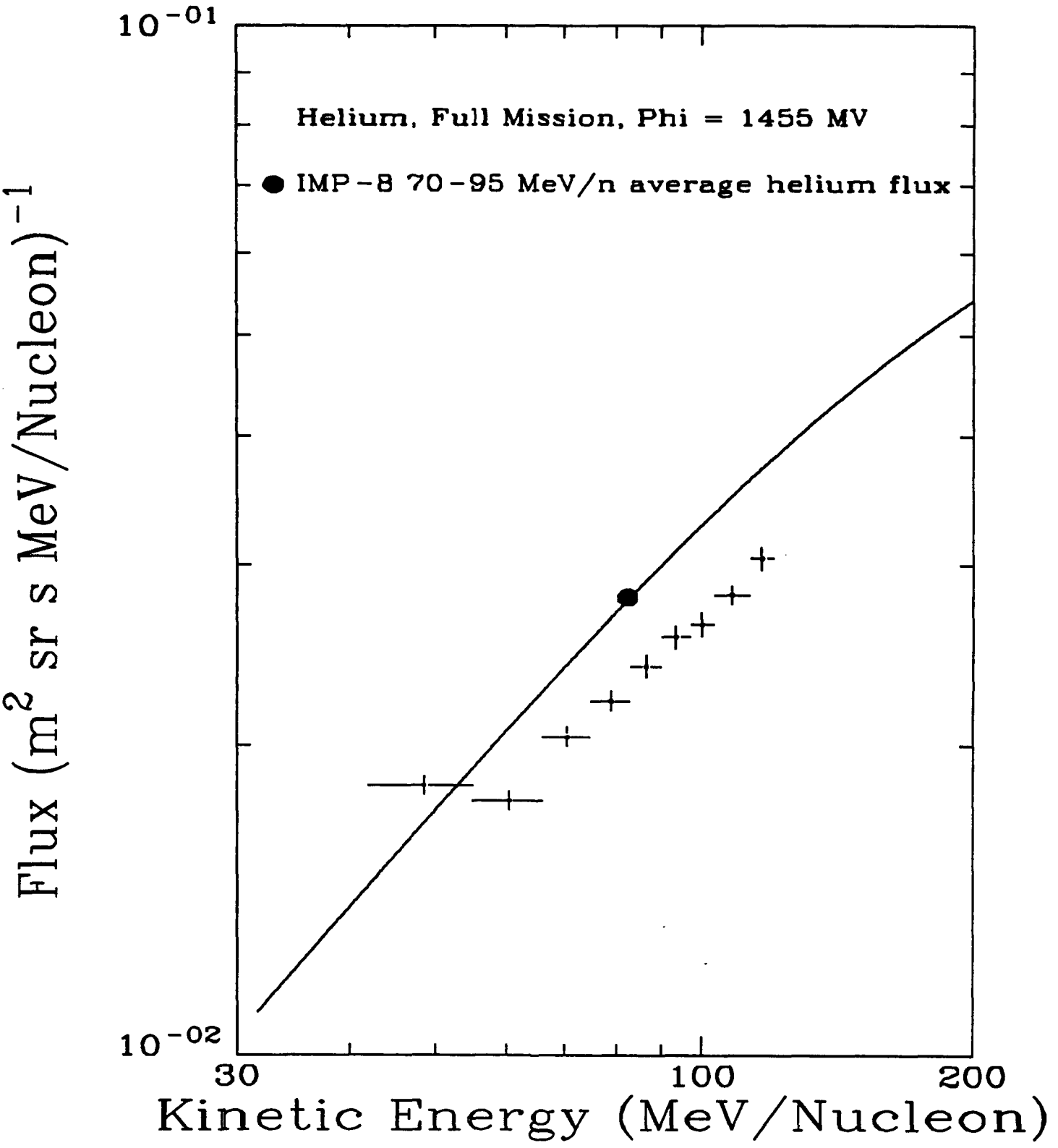

Figure 3. Comparison of first order ONR-604 helium flux measurements (crosses) to predictions (curve) and to IMP-8 helium data.

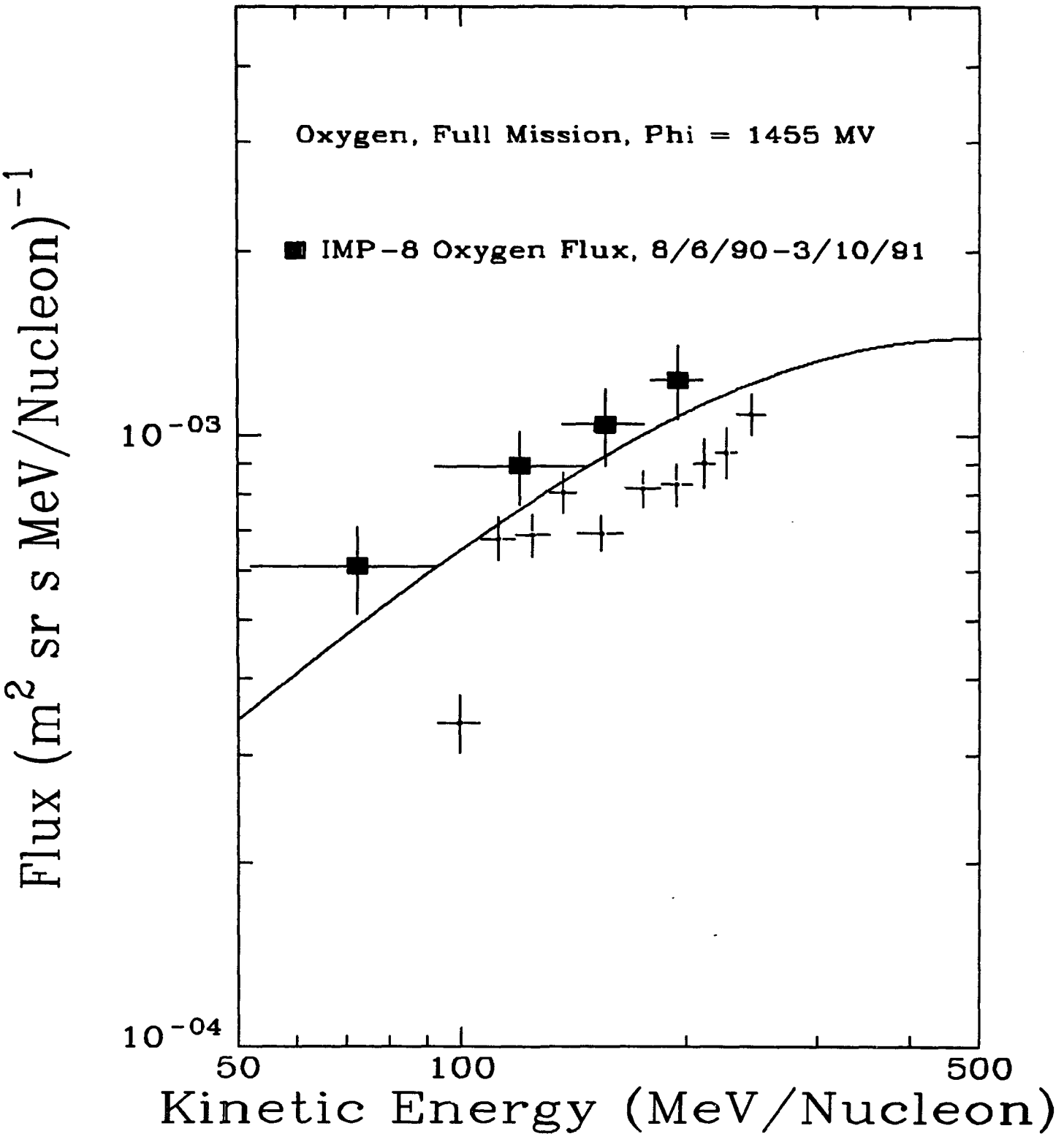

Figure 4. Comparison of first order ONR-604 oxygen flux measurements (crosses) to predictions (curve) and to the IMP-8 oxygen energy spectrum.

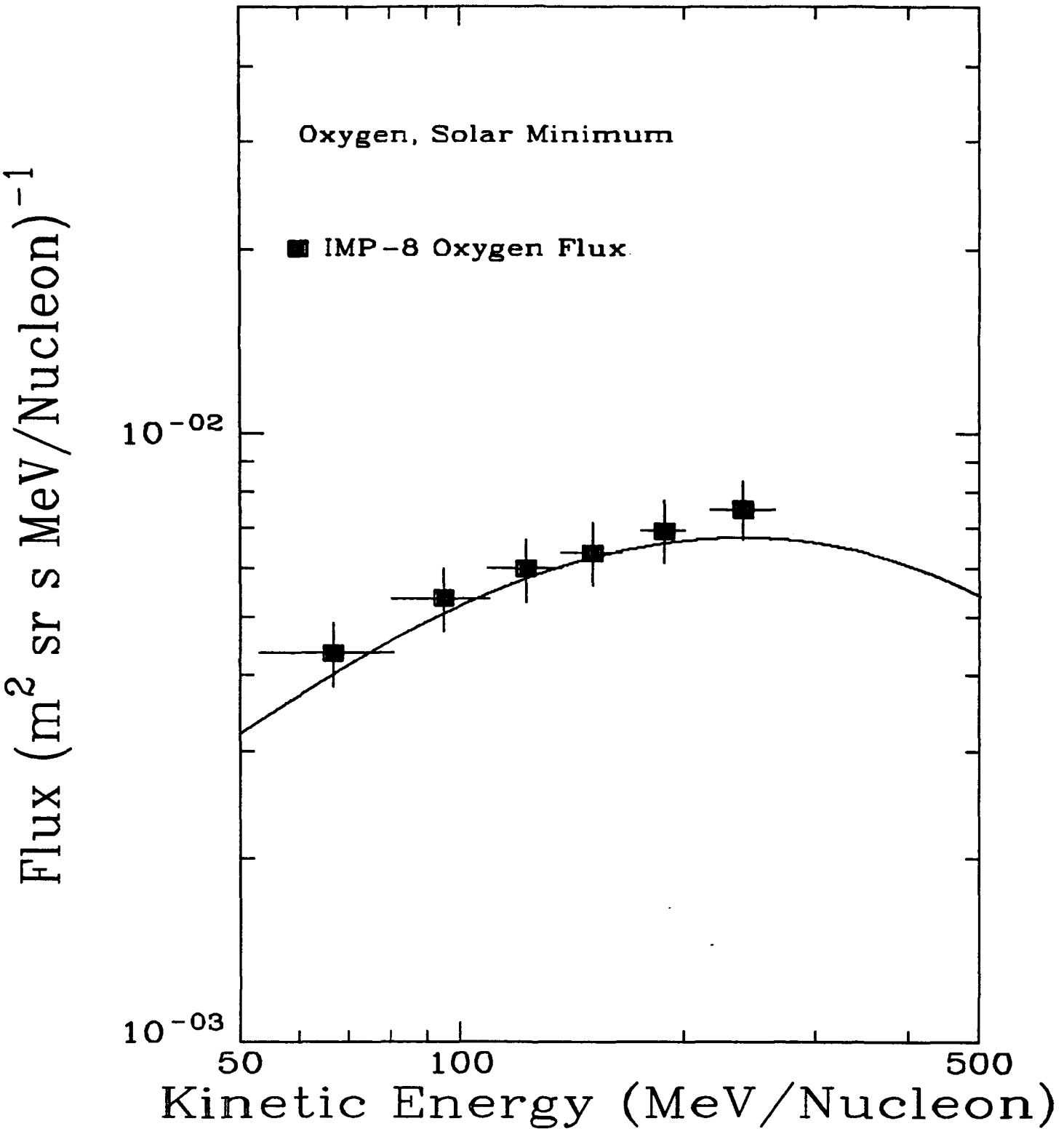

Figure 5. Comparison of IMP-8, solar minimum, oxygen spectrum (Chicago) with predictions.

IV. High Energy Trapped Helium

As discussed in the last report, we have proceeded to prepare a short paper on the observations of the trapped helium by ONR-604 on CRRES. The important conclusions are the two-peak structure, also seen by the SAMPEX spacecraft, and the lack of any correlation with SEP events or the large substorm of March, 1991 as possible sources of origin. Since the high energy trapped helium is seen during 1990 when the anomalous helium is absent from the inner solar system, and based upon the penetration energy required even for singly charged helium, it is not likely that this helium is due to the anomalous component. This manuscript was submitted to Geophysical Research Letters and is being reviewed for possible publication.